Electronic Supplementary Information

Cyclic Arrays of Five Pyrenes on One Rim of a Planar Chiral Pillar[5]arene

Kenichi Kato,*[a] Shunsuke Ohtani,[a] Masayuki Gon,[b] Kazuo Tanaka [b] and Tomoki Ogoshi*[a,c]

[a] Department of Synthetic Chemistry and Biological Chemistry, Graduate School of Engineering, Kyoto University, Nishikyo-ku, Kyoto, 615-8510 (Japan)
E-mail: katok@sbchem.kyoto-u.ac.jp, ogoshi@sbchem.kyoto-u.ac.jp

[b] Department of Polymer Chemistry, Graduate School of Engineering, Kyoto University, Nishikyo-ku, Kyoto, 615-8510 (Japan)

[c] WPI Nano Life Science Institute, Kanazawa University, Kakuma-machi, Kanazawa, 920-1192 (Japan)

Contents

1. General information

Material in Synthesis

All reagents and solvents were of commercial reagent grade and were used without further purification except where noted. Cyclohexylmethyloxy- and hydroxy-substituted pillar[5]arene **9** was prepared according to the reported method.[S1] Dehydrated CH_2Cl_2 (Super²) and dehydrated *N*,*N*-dimethylformamide (DMF, Super) were purchased from Kanto Chemical Co., Inc. Super dehydrated toluene was purchased from Wako Pure Chemical Industry, Ltd. Thin-layer Chromatography (TLC) analyses were performed on commercial aluminium plates bearing a 0.25 mm layer of Merck Silica gel 60 F_{254}. Preparative silica gel chromatography was performed on Wakosil 60 or Wakogel C-400HG. Gel Permeation Chromatography (GPC) was performed on a Japan Analytical Industry LaboACE LC-5060 recycling HPLC apparatus equipped with two JAIGEL-2HR columns, using $CHCl_3$ (containing EtOH) as eluent.

Instrumental

^{1}H (500 MHz) and ^{13}C (126 MHz) NMR spectra were recorded on a JEOL ECZ-500 spectrometer except where noted. Chemical shifts were reported as the delta scale in ppm relative to the internal standards (δ = 7.26 ppm for ^{1}H and 77.16 ppm for ^{13}C in $CDCl_3$.)

High Resolution Atmospheric Pressure Chemical Ionization Fourier Transform (HR-APCI-FT) mass spectra were recorded on a Thermo Fisher Scientific LTQ orbitrap XL instrument by using the APCI method in positive ion mode. Matrix assisted laser desorption/ionization time of fright mass spectrometry (MALDI-TOF-MS) results were recorded on a Bruker Daltonics ultrafleXtreme in the positive ion mode.

Ultraviolet/visible (UV/vis) absorption spectra were recorded on a JASCO V-750 spectrophotometer. Optical separations were performed on a Japan Analytical Industry LaboACE LC-5060 recycling HPLC apparatus equipped with a DAICEL CHIRALPAK IA (ϕ = 20 mm, l = 250 mm) column and the obtained fractions as well as racemic samples were analysed on a Hitachi Chromaster HPLC instrument equipped with a DAICEL CHIRALPAK IA (ϕ = 4.6 mm, l = 250 mm) column. Circular dichroism (CD) spectra were recorded on a JASCO J-1500 spectrometer. Fluorescence spectra were measured on a JASCO FP-8550 spectrofluorometer. Absolute fluorescence quantum yields were determined on a Hamamatsu Photonics Quantaurus-QY C11347 absolute PL quantum yield spectrometer. Circularly polarized luminescence (CPL) spectra were recorded on a JASCO CPL-200 spectrometer. Emission lifetime measurement was performed on a Horiba FluoroCube spectrofluorometer system, and excitation was carried out using a UV diode laser (NanoLED 369 nm). Variable-temperature fluorescence spectra were recorded on a Horiba Fluorolog-3 spectrofluorometer equipped with a cryostat (Thermal Block Company, SA-SB245T) and temperature controller (Oxford, Instruments, ITC 502S).

2. Synthetic procedures and compound data

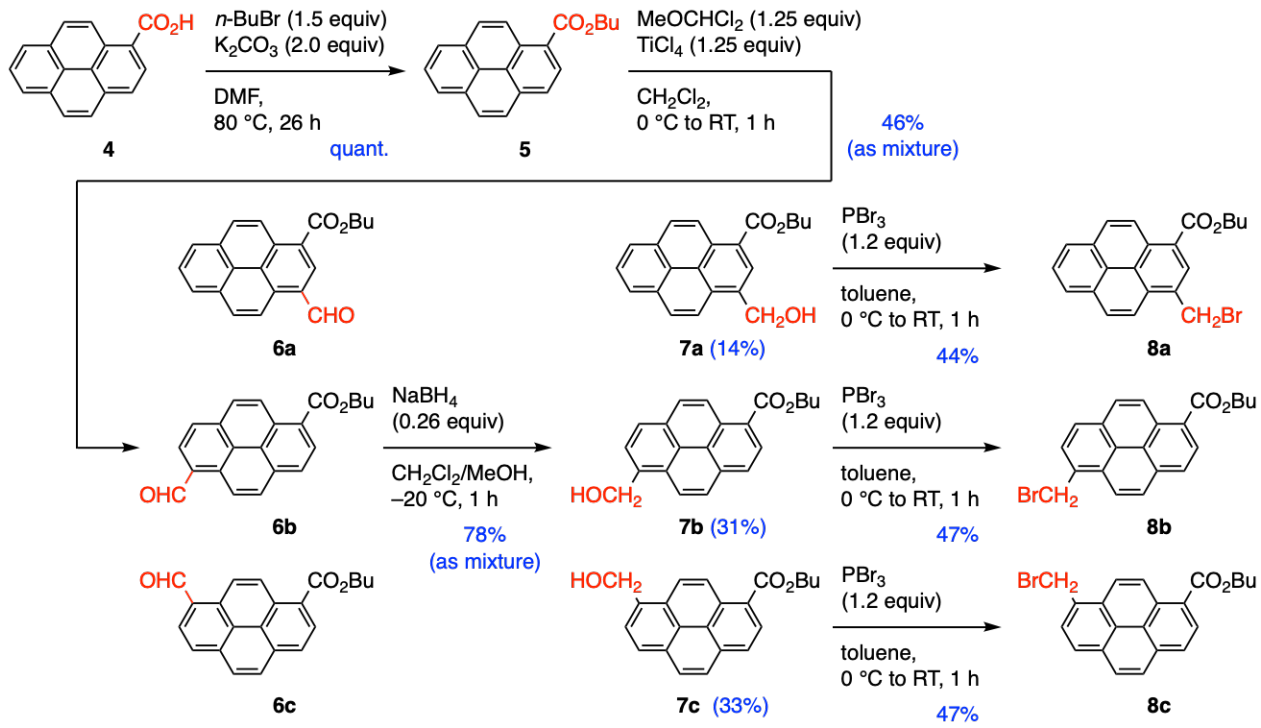

Scheme S2-1. Synthesis of ester-appended 1-(bromomethyl)pyrenes.

Butyl pyrene-1-carboxylate (5): Pyrene-1-carboxylic acid (**4**, 5.22 g, 21 mmol) and K_2CO_3 (5.86 g, 42 mmol) was suspended in DMF (42 mL) in a 100-mL round-bottom flask under nitrogen atmosphere. To the mixture, butyl bromide (3.4 mL, 32 mmol) was slowly added, and the mixture was stirred at 80 °C for 26 h. After solids were removed by filtration, NH_4Cl (aq) was added. The mixture was extracted with a mixture of EtOAc and toluene three times. The organic extract was washed with NH_4Cl (aq) and NaCl (aq) and dried over anhydrous Na_2SO_4. After the solvent was evaporated under reduced pressure, purification by column chromatography on Wakosil 60 (EtOAc/*n*-hexane = 1/8) afforded butyl pyrene-1-carboxylate (**5**, 6.54 g, quant.) as yellow oil. ^{1}H NMR ($CDCl_3$, 298 K): δ / ppm = 9.27 (d, J = 9.0 Hz, 1H, Pyrenyl-H), 8.62 (d, J = 8.0 Hz, 1H, Pyrenyl-H), 8.26–8.21 (m, 3H, Pyrenyl-H), 8.16–8.13 (m, 2H, Pyrenyl-H), 8.07–8.02 (m, 2H, Pyrenyl-H), 4.53 (t, J = 6.5 Hz, 2H, $C\underline{H}_2CH_2CH_2CH_3$), 1.92–1.87 (m, 2H, $CH_2C\underline{H}_2CH_2CH_3$), 1.63–1.56 (m, 2H, $CH_2CH_2C\underline{H}_2CH_3$), and 1.06 (t, J = 7.5 Hz, 3H,$CH_2CH_2CH_2C\underline{H}_3$); ^{13}C NMR ($CDCl_3$, 298 K): δ / ppm = 168.27, 134.33, 131.19, 131.12, 130.51, 129.64, 129.46, 128.46, 127.28, 126.38, 126.33, 126.23, 125.06, 124.95, 124.33, 124.22, 124.04, 65.25, 31.07, 19.61, and 13.99; HR-APCI-FT-MS (positive): m/z calcd for $[C_{21}H_{19}O_2]^+$: 303.1380 $[M+H]^+$; found: 303.1383.

Butyl formylpyrene-1-carboxylate (6): Butyl pyrene-1-carboxylate (**5**, 6.54 g, 21 mmol) was dissolved in CH_2Cl_2 (162 mL) in a 200-mL round-bottom flask under nitrogen atmosphere. After dichloromethyl methyl ether (2.4 mL, 27 mmol) was introduced, the solution was cooled to 0 °C with an ice bath. Then, $TiCl_4$ (3.0 mL,

27 mmol) was slowly added. The mixture was allowed to warm up to room temperature and stirred for 14 h. The mixture was quenched with ice and deionized water and extracted with CH_2Cl_2 three times. The organic extract was washed with $NaHCO_3$ (aq) and dried over anhydrous Na_2SO_4. After the solvent was evaporated under reduced pressure, purification by column chromatography on Wakogel C-400HG (CH_2Cl_2/*n*-hexane = 1/1 to 1/0) afforded a mixture of butyl 3-formylpyrene-1-carboxylate (**6a**), butyl 6-formylpyrene-1-carboxylate (**6b**), and butyl 8-formylpyrene-1-carboxylate (**6c**) as yellow solids (total 3.30 g, 10 mmol, 46%). Starting material was also recovered (2.0 g, 30%). ^{1}H NMR ($CDCl_3$, 400 MHz, 298 K): δ / ppm = 10.88 (s, 1H, C<u>H</u>O of 1,6- or 1,8-isomer), 10.82 (s, 1H, C<u>H</u>O of 1,6- or 1,8-isomer), 10.77 (s, 1H, C<u>H</u>O of 1,3-isomer **6a**), 9.58–9.35 (m, 2H, Pyrenyl-H), 9.09 (s, 1H, 2-Pyrenyl-H of 1,3-isomer **6a**), 8.69 (m, 1H, Pyrenyl-H), 8.53 (m, 1H, Pyrenyl-H), 8.47–8.16 (m, 4H, Pyrenyl-H), 4.58–4.52 (m, 2H, C<u>H</u>$_2$CH$_2$CH$_2$CH$_3$), 1.95–1.88 (m, 2H, CH$_2$C<u>H</u>$_2$CH$_2$CH$_3$), 1.63–1.58 (m, 2H, CH$_2$CH$_2$C<u>H</u>$_2$CH$_3$), and 1.06 (t, *J* = 9.0 Hz, 3H,CH$_2$CH$_2$CH$_2$C<u>H</u>$_3$); ^{13}C NMR ($CDCl_3$, 298 K): δ / ppm = 193.10, 192.93, 192.79, 167.87, 167.30, 135.37, 135.05, 134.81, 134.62, 133.96, 133.41, 133.22, 132.92, 132.77, 132.60, 131.74, 131.20, 130.97, 130.87, 130.55, 130.40, 130.31, 130.27, 130.02, 129.27, 129.07, 128.98, 128.84, 128.35, 128.25, 128.19, 127.05, 126.40, 126.18, 126.05, 125.99, 125.87, 125.83, 125.69, 125.06, 124.83, 124.59, 124.40, 124.33, 123.05, 65.68, 65.61, 65.57, 31.04, 19.60, and 13.99; HR-APCI-FT-MS (positive): *m*/*z* calcd for $[C_{21}H_{19}O_3]^+$: 331.1329 $[M+H]^+$; found: 331.1335.

Butyl (hydroxymethyl)pyrene-1-carboxylate (7): Butyl formylpyrene-1-carboxylate (**6**, 3.30 g, 10 mmol) was suspended in a mixture of CH_2Cl_2 (80 mL) and MeOH (80 mL) in a 300-mL round-bottom flask. The mixture was cooled to –20 °C using ice and NaCl, to which $NaBH_4$ (98 mg, 2.6 mmol) was added portionwise. The mixture was stirred for 1 h. After NH_4Cl (aq) was added, the mixture was warmed up to room temperature. The mixture was extracted with CH_2Cl_2 three times. The organic extract was dried over anhydrous Na_2SO_4 and the solvent was evaporated under reduced pressure. Purification by column chromatography on Wakogel C-400HG (CH_2Cl_2/*n*-hexane = 1/1 to 1/0, then 0-10% acetone was added) afforded a mixture of butyl 3-(hydroxymethyl)pyrene-1-carboxylate (**7**) as yellow solids. The mixture was further separated on a recycling HPLC apparatus equipped with a chiral column (eluent: CH_2Cl_2/*n*-hexane = 1/2), giving butyl 3-(hydroxymethyl)pyrene-1-carboxylate (**7a**, 454 mg, 1.4 mmol, 14%), butyl 6-(hydroxymethyl)pyrene-1-carboxylate (**7b**, 1.04 g, 3.1 mmol, 31%), and butyl 8-(hydroxymethyl)pyrene-1-carboxylate (**7c**, 1.10 g, 3.3 mmol, 33%).

<u>Compound data of **7a**</u>: ^{1}H NMR ($CDCl_3$, 298 K): δ / ppm = 8.96 (d, *J* = 9.0 Hz, 1H, Pyrenyl-H), 8.43 (s, 1H, 2-Pyrenyl-H), 8.08–7.87 (m, 6H, Pyrenyl-H), 5.18 (br, 2H, C<u>H</u>$_2$OH), 4.44 (t, *J* = 6.8 Hz, 2H, C<u>H</u>$_2$CH$_2$CH$_2$CH$_3$), 2.68 (br, 1H, CH$_2$O<u>H</u>), 1.87–1.80 (m, 2H, CH$_2$C<u>H</u>$_2$CH$_2$CH$_3$), 1.58–1.52 (m, 2H, CH$_2$CH$_2$C<u>H</u>$_2$CH$_3$), and 1.03 (t, *J* = 7.5 Hz, 3H, CH$_2$CH$_2$CH$_2$C<u>H</u>$_3$); ^{13}C NMR ($CDCl_3$, 298 K): δ / ppm = 168.27, 132.81, 131.51, 130.64, 130.41, 130.25, 129.64, 129.09, 127.72, 126.43, 126.97, 126.18, 124.80, 124.52, 123.98, 123.10, 122.45, 65.32, 63.50, 30.98, 19.52, and 13.97; HR-APCI-FT-MS (positive): *m*/*z* calcd for $[C_{22}H_{19}O_2]^+$: 315.1380 $[M–OH]^+$; found: 315.1386.

Compound data of **7b**: ^{1}H NMR ($CDCl_3$, 298 K): δ / ppm = 8.96 (d, J = 9.0 Hz, 1H, Pyrenyl-H), 8.43 (d, J = 8.0 Hz, 1H, Pyrenyl-H), 8.06 (d, J = 9.5 Hz, 1H, Pyrenyl-H), 7.91–7.86 (m, 3H, Pyrenyl-H), 7.83 (d, J = 8.0 Hz, 1H, Pyrenyl-H), 7.75 (d, J = 9.5 Hz, 1H, Pyrenyl-H), 5.16 (br, 2H, $C\underline{H}_2OH$), 4.49 (t, J = 6.8 Hz, 2H, $C\underline{H}_2CH_2CH_2CH_3$), 2.77 (br, 1H, $CH_2O\underline{H}$), 1.92–1.85 (m, 2H, $CH_2C\underline{H}_2CH_2CH_3$), 1.63–1.55 (m, 2H, $CH_2CH_2C\underline{H}_2CH_3$), and 1.06 (t, J = 7.5 Hz, 3H, $CH_2CH_2CH_2C\underline{H}_3$); ^{13}C NMR ($CDCl_3$, 298 K): δ / ppm = 168.34, 135.02, 133.51, 130.96, 129.96, 129.15, 128.20, 128.10, 127.14, 125.87, 125.65, 124.75, 124.55, 124.43, 124.11, 124.04, 123.77, 65.28, 63.45, 30.99, 19.55, and 13.96; HR-APCI-FT-MS (positive): m/z calcd for $[C_{22}H_{19}O_2]^+$: 315.1380 $[M–OH]^+$; found: 315.1387.

Compound data of **7c**: ^{1}H NMR ($CDCl_3$, 298 K): δ / ppm = 9.20 (d, J = 9.8 Hz, 1H, Pyrenyl-H), 8.57 (d, J = 8.0 Hz, 1H, Pyrenyl-H), 8.36 (d, J = 9.8 Hz, 1H, Pyrenyl-H), 8.12–8.08 (m, 2H, Pyrenyl-H), 8.05–8.01 (m, 2H, Pyrenyl-H), 7.96 (d, J = 8.8 Hz, 1H, Pyrenyl-H), 5.37 (br, 2H, $C\underline{H}_2OH$), 4.52 (t, J = 6.8 Hz, 2H, $C\underline{H}_2CH_2CH_2CH_3$), 2.20 (br, 1H, $CH_2O\underline{H}$), 1.93–1.87 (m, 2H, $CH_2C\underline{H}_2CH_2CH_3$), 1.64–1.55 (m, 2H, $CH_2CH_2C\underline{H}_2CH_3$), and 1.06 (t, J = 7.5 Hz, 3H, $CH_2CH_2CH_2C\underline{H}_3$); ^{13}C NMR ($CDCl_3$, 298 K): δ / ppm = 168.29, 135.18, 134.41, 130.97, 130.64, 129.62, 128.51, 127.85, 127.16, 126.09, 125.31, 124.95, 124.78, 124.43, 124.14, 65.33, 63.58, 31.06, 19.61, and 14.00; HR-APCI-FT-MS (positive): m/z calcd for $[C_{22}H_{19}O_2]^+$: 315.1380 $[M–OH]^+$; found: 315.1387.

General procedure for bromination of butyl (hydroxymethyl)pyrene-1-carboxylate: Butyl (hydroxymethyl)pyrene-1-carboxylate was dissolved in toluene in a round-bottom flask under nitrogen atmosphere. The mixture was cooled to 0 °C with an ice bath, to which PBr_3 was dropwise added. After stirring for 1 h, the mixture was warmed up to room temperature. The mixture was quenched with $NaHCO_3$ (aq) and extracted with CH_2Cl_2 three times. The organic extract was dried over anhydrous Na_2SO_4, and the solvent was evaporated under reduced pressure. Purification by column chromatography on Wakogel C-400HG (CH_2Cl_2/*n*-hexane = 1/3 to 1/1) afforded corresponding butyl (bromomethyl)pyrene-1-carboxylate.

Butyl 3-(bromomethyl)pyrene-1-carboxylate (8a): According to **General procedure for bromination of butyl (hydroxymethyl)pyrene-1-carboxylate**, butyl 3-(hydroxymethyl)pyrene-1-carboxylate (**7a**, 274 mg, 0.82 mmol) was reacted with PBr_3 (0.094 mL, 0.99 mmol) in toluene (8.2 mL), giving butyl 3-(bromomethyl) pyrene-1-carboxylate (**8a**, 144 mg, 0.36 mmol, 44%) as yellow solids. ^{1}H NMR ($CDCl_3$, 298 K): δ / ppm = 9.24 (d, J = 9.5 Hz, 1H, Pyrenyl-H), 8.65 (s, 1H, Pyrenyl-H), 8.41 (d, J = 9.0 Hz, 1H, Pyrenyl-H), 8.35–8.29 (m, 3H, Pyrenyl-H), 8.24 (d, J = 9.5 Hz, 1H, Pyrenyl-H), 8.09 (d, J = 7.5 Hz, 1H, Pyrenyl-H), 5.25 (s, 2H, $C\underline{H}_2Br$), 4.53 (t, J = 6.5 Hz, 2H, $C\underline{H}_2CH_2CH_2CH_3$), 1.94–1.88 (m, 2H, $CH_2C\underline{H}_2CH_2CH_3$), 1.63–1.55 (m, 2H, $CH_2CH_2C\underline{H}_2CH_3$), and 1.06 (t, J = 7.3 Hz, 3H, $CH_2CH_2CH_2C\underline{H}_3$); ^{13}C NMR ($CDCl_3$, 298 K): δ / ppm = 167.75, 132.24, 131.88, 130.82, 130.65, 130.47, 130.18, 130.08, 129.85, 127.10, 126.96, 126.85, 125.73, 125.04, 124.41, 123.97, 122.87, 65.52, 31.93, 31.07, 19.61, and 14.01; HR-APCI-FT-MS (positive): m/z calcd for $[C_{22}H_{20}{}^{79}Br_1O_2]^+$: 395.0641 $[M–H]^+$; found: 395.0646.

Butyl 6-(bromomethyl)pyrene-1-carboxylate (8b): According to **General procedure for bromination of butyl (hydroxymethyl)pyrene-1-carboxylate**, butyl 6-(hydroxymethyl)pyrene-1-carboxylate (**7b**, 639 mg, 1.9 mmol) was reacted with PBr_3 (0.18 mL, 2.3 mmol) in toluene (19 mL), giving butyl 6-(bromomethyl)pyrene-1-carboxylate (**8b**, 353 mg, 0.89 mmol, 47%) as yellow solids. ^{1}H NMR ($CDCl_3$, 298 K): δ / ppm = 9.23 (d, J = 9.0 Hz, 1H, Pyrenyl-H), 8.61 (d, J = 8.0 Hz, 1H, Pyrenyl-H), 8.45 (d, J = 9.0 Hz, 1H, Pyrenyl-H), 8.21–8.17 (m, 2H, Pyrenyl-H), 8.16–8.13 (m, 2H, Pyrenyl-H), 8.03 (d, J = 8.0 Hz, 1H, Pyrenyl-H), 5.23 (s, 2H, $C\underline{H}_2Br$), 4.52 (t, J = 6.8 Hz, 2H, $C\underline{H}_2CH_2CH_2CH_3$), 1.93–1.87 (m, 2H, $CH_2C\underline{H}_2CH_2CH_3$), 1.64–1.56 (m, 2H, $CH_2CH_2C\underline{H}_2CH_3$), and 1.06 (t, J = 7.5 Hz, 3H, $CH_2CH_2CH_2C\underline{H}_3$); ^{13}C NMR ($CDCl_3$, 298 K): δ / ppm = 168.18, 133.82, 132.00, 131.26, 131.24, 129.38, 129.11, 128.74, 128.23, 128.07, 126.12, 125.61, 124.96, 124.93, 124.87, 124.69, 65.39, 31.89, 31.06, 19.61, and 14.00; HR-APCI-FT-MS (positive): m/z calcd for $[C_{22}H_{20}{}^{79}Br_1O_2]^+$: 395.0641 $[M–H]^+$; found: 395.0653.

Butyl 8-(bromomethyl)pyrene-1-carboxylate (8c): According to **General procedure for bromination of butyl (hydroxymethyl)pyrene-1-carboxylate**, butyl 8-(hydroxymethyl)pyrene-1-carboxylate (**7c**, 810 mg, 2.4 mmol) was reacted with PBr_3 (0.23 mL, 2.9 mmol) in toluene (24 mL), giving butyl 8-(bromomethyl)pyrene-1-carboxylate (**8c**, 451 mg, 1.1 mmol, 47%) as off-white solids. ^{1}H NMR ($CDCl_3$, 298 K): δ / ppm = 9.38 (d, J = 10 Hz, 1H, Pyrenyl-H), 8.62 (d, J = 8.5 Hz, 1H, Pyrenyl-H), 8.49 (d, J = 9.5 Hz, 1H, Pyrenyl-H), 8.18–8.12 (m, 2H, Pyrenyl-H), 8.09–8.00 (m, 3H, Pyrenyl-H), 5.24 (s, 2H, $C\underline{H}_2Br$), 4.53 (t, J = 6.5 Hz, 2H, $C\underline{H}_2CH_2CH_2CH_3$), 1.94–1.88 (m, 2H, $CH_2C\underline{H}_2CH_2CH_3$), 1.64–1.58 (m, 2H, $CH_2CH_2C\underline{H}_2CH_3$), and 1.06 (t, J = 7.5 Hz, 3H, $CH_2CH_2CH_2C\underline{H}_3$); ^{13}C NMR ($CDCl_3$, 298 K): δ / ppm = 168.13, 134.36, 132.01, 131.90, 130.70, 129.56, 128.83, 128.44, 128.17, 127.88, 126.24, 125.87, 124.98, 124.87, 124.78, 124.71, 65.39, 31.67, 31.08, 19.61, and 14.01; HR-APCI-FT-MS (positive): m/z calcd for $[C_{22}H_{20}{}^{79}Br_1O_2]^+$: 395.0641 $[M–H]^+$; found: 395.0649.

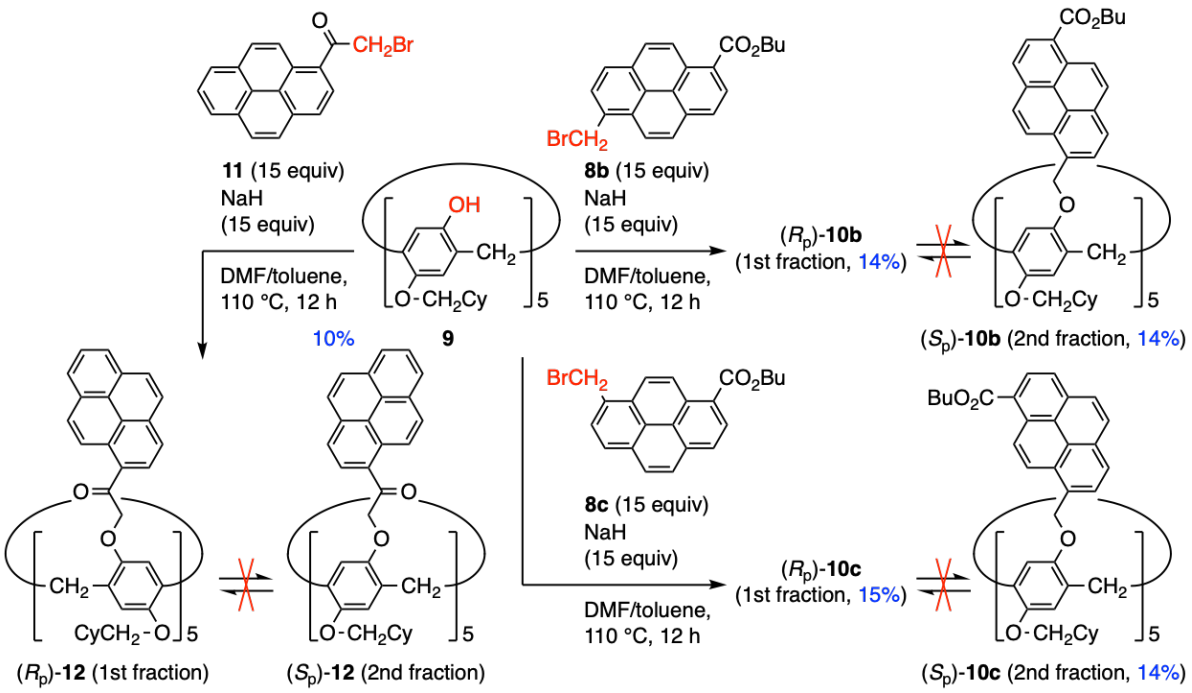

Scheme S2-2. Synthesis of rim-differentiated pillar[5]arenes bearing pyrene rings on one side.

General procedure for installation of pyrenyl groups onto the rim of pillar[5]arene: NaH (60% dispersion, 14 mg, 0.34 mmol) was suspended in a mixture of DMF (20 mL) and toluene (10 mL) in a 100-mL round-bottom flask under nitrogen atmosphere. To the mixture, pillar[5]arene **9**[S1] (25 mg, 0.023 mmol) and then butyl (bromomethyl)pyrene-1-carboxylate (**8**, 136 mg, 0.34 mmol) were added. The mixture was stirred at 110 °C for 12-14 h. The mixture was quenched with NH_4Cl (aq) and extracted with CH_2Cl_2 three times. The organic extract was washed with NH_4Cl (aq) and passed through a short column of anhydrous Na_2SO_4 and Wakosil 60. After the solvent was evaporated under reduced pressure, purification by column chromatography on Wakogel C-400HG (CH_2Cl_2/*n*-hexane = 1/1 to 1/0) afforded a mixture of target pillar[5]arene **7** and ester-substituted pyrenes. The mixture was further separated on a recycling HPLC apparatus equipped with a chiral column (eluent: CH_2Cl_2/*n*-hexane = 1/1), giving pillar[5]arene **10**.

Cyclohexylmethyloxy- and [3-(butoxycarbonyl)pyren-1-yl]methoxy-substituted pillar[5]arene 10a: According to **General procedure for installation of pyrenyl groups onto the rim of pillar[5]arene**, pillar[6]arene **9** was reacted with 3-(bromomethyl)pyrene-1-carboxylate, but no product was obtained after careful column chromatography.

Cyclohexylmethyloxy- and [6-(ethoxycarbonyl)pyren-1-yl]methoxy-substituted pillar[5]arene 10b: According to **General procedure for installation of pyrenyl groups onto the rim of pillar[5]arene**, pillar[6]arene **9** was reacted with 6-(bromomethyl)pyrene-1-carboxylate, giving (R_P)-**10b** (1st fraction, >98%ee, 9.3 mg, 0.0035 mmol, 15%) and (S_P)-**10b** (2nd fraction, 95%ee, 8.5 mg, 0.0032 mmol, 14%) as yellow solids. ^{1}H

NMR ($CDCl_3$, 298 K): δ / ppm = 8.80 (d, J = 9.0 Hz, 1H, Pyrenyl-H), 8.20 (d, J = 8.5 Hz, 1H, Pyrenyl-H), 8.00–7.77 (m, 2H, Pyrenyl-H), 7.75 (d, J = 7.5 Hz, 1H, Pyrenyl-H), 7.33 (d, J = 8.0 Hz, 1H, Pyrenyl-H), 7.24 (d, J = 9.5 Hz, 1H, Pyrenyl-H), 7.17 (s, 1H, Pillar[5]arene-H), 6.98 (s, 1H, Pillar[5]arene-H), 6.87 (d, J = 9.0 Hz, 1H, Pyrenyl-H), 5.04 (d, J = 13 Hz, 1H, Pyrenyl-C$\underline{H}_2$O), 4.86 (d, J = 13 Hz, 1H, Pyrenyl-C$\underline{H}_2$O), 4.41 (t, J = 6.8 Hz, 2H, C$\underline{H}_2$CH$_2$CH$_2$CH$_3$), 3.99–3.90 (m, 3H, Pillar[5]arene-C$\underline{H}_2$ and CyC$\underline{H}_2$O), 3.65 (t, J = 7.8 Hz, 1H, CyC$\underline{H}_2$O), 2.10 (d, J = 11 Hz, 1H, Cy-H), 2.02 (d, J = 11 Hz, 1H, Cy-H), 1.93–1.78 (m, 6H, Cy-H and CH$_2$C$\underline{H}_2$CH$_2$CH$_3$), 1.62–1.55 (m, 2H, CH$_2$CH$_2$C$\underline{H}_2$CH$_3$), 1.40–1.18 (m, 5H, Cy-H), and 1.07 (t, J = 7.5 Hz, 3H, CH$_2$CH$_2$CH$_2$C$\underline{H}_3$); ^{13}C NMR ($CDCl_3$, 298 K): δ / ppm = 167.78, 150.71, 149.86, 133.17, 131.98, 131.00, 129.92, 129.21, 128.96, 128.51, 128.04, 127.71, 126.98, 125.57, 125.40, 124.57, 124.42, 124.03, 123.92, 123.66, 115.58, 114.89, 74.11, 68.59, 65.08, 38.74, 31.07, 30.65, 30.44, 29.67, 26.85, 26.29, 26.25, 19.61, and 14.04; MALDI-TOF-MS (positive): m/z calcd for $[C_{180}H_{180}O_{20}Na]^+$: 2684.296 $[M+Na]^+$; found: 2684.294; UV/vis ($CHCl_3$): λ_{max} / nm (ε / M^{-1} cm^{-1}) = 286 (1.4×10^5), 358 (1.2 ×10^5), and 389 (4.9×10^4); FL ($CHCl_3$, Φ_{lum} = 0.13): λ_{max} / nm = 396 and 417; 1st fraction (>98%ee): CD ($CHCl_3$): λ_{max} / nm ($\Delta\varepsilon$ / M^{-1} cm^{-1}, g_{abs}) = 251 (140, 1.2×10^{-3}), 276 (34, 0.4×10^{-3}), 291 (–40, –0.4×10^{-3}), 310 (130, 4.1×10^{-3}), and 372 (79, 1.0×10^{-3}); 2nd fraction (95%ee): CD ($CHCl_3$): λ_{max} / nm ($\Delta\varepsilon$ / M^{-1} cm^{-1}, g_{abs}) = 251 (–140, –1.3×10^{-3}), 274 (–38, –0.4×10^{-3}), 290 (39, 0.4×10^{-3}), 310 (–120, –3.9×10^{-3}), and 370 (–86, –1.0×10^{-3}).

Cyclohexylmethyloxy- and [8-(ethoxycarbonyl)pyren-1-yl]methoxy-substituted pillar[5]arene 10c: According to **General procedure for installation of pyrenyl groups onto the rim of pillar[5]arene**, pillar[6]arene **9** was reacted with 8-(bromomethyl)pyrene-1-carboxylate, giving (R_P)-**10c** (1st fraction, >98%ee, 8.6 mg, 0.0032 mmol, 14%) and (S_P)-**10c** (2nd fraction, 97%ee, 8.7 mg, 0.0033 mmol, 14%) as yellow solids. ^{1}H NMR ($CDCl_3$, 298 K): δ / ppm = 9.00 (d, J = 10 Hz, 1H, Pyrenyl-H), 8.37 (d, J = 8.0 Hz, 1H, Pyrenyl-H), 7.97 (d, J = 9.5 Hz, 1H, Pyrenyl-H), 7.79–7.74 (m, 3H, Pyrenyl-H), 7.67 (d, J = 9.0 Hz, 1H, Pyrenyl-H), 7.55 (d, J = 9.0 Hz, 1H, Pyrenyl-H), 7.02 (s, 1H, Pillar[5]arene-H), 6.93 (s, 1H, Pillar[5]arene-H), 5.02 (d, J = 12 Hz, 1H, Pyrenyl-C$\underline{H}_2$O), 4.93 (d, J = 12 Hz, 1H, Pyrenyl-C$\underline{H}_2$O), 4.35 (t, J = 6.5 Hz, 2H, C$\underline{H}_2$CH$_2$CH$_2$CH$_3$), 3.90–3.83 (m, 3H, Pillar[5]arene-C$\underline{H}_2$ and CyC$\underline{H}_2$O), 3.59 (t, J = 7.8 Hz, 1H, CyC$\underline{H}_2$O), 2.06 (d, J = 12 Hz, 1H, Cy-H), 1.96 (d, J = 12 Hz, 1H, Cy-H), 1.89–1.74 (m, 6H, Cy-H and CH$_2$C$\underline{H}_2$CH$_2$CH$_3$), 1.53–1.46 (m, 2H, CH$_2$CH$_2$C$\underline{H}_2$CH$_3$), 1.39–1.13 (m, 5H, Cy-H), and 0.97 (t, J = 7.5 Hz, 3H, CH$_2$CH$_2$CH$_2$C$\underline{H}_3$); ^{13}C NMR ($CDCl_3$, 298 K): δ / ppm = 167.80, 150.68, 149.82, 134.21, 132.28, 130.81, 130.58, 129.47, 128.86, 128.48, 128.29, 128.01, 126.81, 126.69, 125.85, 125.11, 124.89, 124.69, 124.17, 124.09, 123.71, 115.71, 115.05, 74.22, 68.76, 65.04, 38.68, 31.01, 30.62, 30.38, 29.87, 29.62, 26.85, 26.26, 26.22, 19.54, and 13.97; HR-APCI-FT-MS (positive): m/z calcd for $[C_{180}H_{181}O_{20}]^+$: 2662.3141 $[M+H]^+$; found: 2662.3057; UV/vis ($CHCl_3$): λ_{max} / nm (ε / M^{-1} cm^{-1}) = 286 (1.5×10^5), 358 (1.2 ×10^5), and 389 (5.3×10^4); FL ($CHCl_3$, Φ_{lum} = 0.15): λ_{max} / nm = 397 and 417; 1st fraction (>98%ee): CD ($CHCl_3$): λ_{max} / nm ($\Delta\varepsilon$ / M^{-1} cm^{-1}, g_{abs}) = 252 (92, 0.9×10^{-3}), 279 (52, 0.4×10^{-3}), 290 (–24, –0.2×10^{-3}), 310 (120, 3.7×10^{-3}), and 361 (41, 0.3×10^{-3}); CPL ($CHCl_3$): λ_{max} / nm (g_{lum}) = ca. 500 (–2.9×10^{-3}); 2nd fraction (97%ee): CD ($CHCl_3$): λ_{max} / nm ($\Delta\varepsilon$ / M^{-1} cm^{-1}, g_{abs}) = 253 (–90, –0.9×10^{-3}), 279 (–56, –0.5×10^{-3}), 290 (22, 0.2×10^{-3}), 310 (–110, –3.5×10^{-3}), and 354 (–39, –

0.3×10^{-3}); CPL ($CHCl_3$): λ_{max} / nm (g_{lum}) = ca. 500 (3.5×10^{-3}).

Cyclohexylmethyloxy- and (pyrene-1-carbonyl)methoxy-substituted pillar[5]arene 12: NaH (60% dispersion, 14 mg, 0.34 mmol) was suspended in a mixture of DMF (20 mL) and toluene (10 mL) in a 100-mL round-bottom flask under nitrogen atmosphere. To the mixture, pillar[5]arene **9**[S1] (25 mg, 0.023 mmol) and then 1-(bromoacetyl)pyrene (**11**, 111 mg, 0.34 mmol) were added. The mixture was stirred at 110 °C for 12 h. The mixture was quenched with NH_4Cl (aq) and extracted with CH_2Cl_2 three times. The organic extract was washed with NH_4Cl (aq) and passed through a short column of anhydrous Na_2SO_4 and Wakosil 60. After the solvent was evaporated under reduced pressure, separation by column chromatography on Wakogel C-400HG (CH_2Cl_2/*n*-hexane = 1/1 to 1/0) afforded a mixture containing target pillar[5]arene **12**. The mixture was further purified on a recycling HPLC apparatus equipped with GPC columns (eluent: $CHCl_3$), which was recrystallized from CH_2Cl_2/*n*-hexane to give racemic pillar[5]arene **12** (5.3 mg, 0.0023 mmol, 10%) as yellow solids. ^{1}H NMR ($CDCl_3$, 298 K): δ / ppm = 8.64 (d, *J* = 9.0 Hz, 1H, Pyrenyl-H), 8.01 (d, *J* = 8.0 Hz, 1H, Pyrenyl-H), 7.87 (s, 1H, Pillar[5]arene-H), 7.78 (d, *J* = 7.5 Hz, 1H, Pyrenyl-H), 7.61 (t, *J* = 7.5 Hz, 1H, Pyrenyl-H), 7.38 (d, *J* = 7.5 Hz, 1H, Pyrenyl-H), 7.27 (d, *J* = 9.0 Hz, 1H, Pyrenyl-H), 7.21 (d, *J* = 9.0 Hz, 1H, Pyrenyl-H), 7.08 (s, 1H, Pillar[5]arene-H), 6.00 (d, *J* = 8.0 Hz, 1H, Pyrenyl-H), 5.90–5.85 (m, 2H, Pyrenyl-H and Pyrenyl-C$\underline{H}_2$O), 5.49 (d, *J* = 18 Hz, 1H, Pyrenyl-C$\underline{H}_2$O), 4.22 (d, *J* = 14 Hz, 1H, Pillar[5]arene-C$\underline{H}_2$), 4.04–3.98 (m, 2H, Pillar[5]arene-C$\underline{H}_2$ and CyC$\underline{H}_2$O), 3.68 (t, *J* = 7.5 Hz, 1H, CyC$\underline{H}_2$O), 2.18 (d, *J* = 12 Hz, 1H, Cy-H), 2.07–1.80 (m, 5H, Cy-H), and 1.47–1.13 (m, 5H, Cy-H); ^{13}C NMR ($CDCl_3$, 298 K): δ / ppm = 198.35, 150.78, 148.99, 133.02, 130.39, 129.75, 129.46, 129.03, 128.79, 128.70, 128.53, 125.91, 125.84, 125.73, 125.68, 125.49, 124.48, 124.09, 123.62, 123.33, 115.43, 115.09, 74.37, 72.15, 38.81, 30.74, 30.43, 29.63, 26.94, 26.35, and 26.30; HR-APCI-FT-MS (positive): *m*/*z* calcd for $[C_{160}H_{141}O_{15}]^+$: 2302.0265 $[M+H]^+$; found: 2302.0283; UV/vis ($CHCl_3$): λ_{max} / nm (ε / M^{-1} cm^{-1}) = 288 (1.2×10^5) and 356 (9.0×10^4); FL ($CHCl_3$, 4.4×10^{-6} M, Φ_{lum} = 0.01): λ_{max} / nm = 394, 415, and 547; 1st fraction (>98%ee): CD ($CHCl_3$): λ_{max} / nm ($\Delta\varepsilon$ / M^{-1} cm^{-1}, g_{abs}) = 287 (–140, –1.1×10^{-3}), 310 (160, 4.7×10^{-3}), 347 (–62, –0.8×10^{-3}), and 373 (98, 1.5×10^{-3}); CPL ($CHCl_3$): λ_{max} / nm (g_{lum}) = ca. 547 (6.8×10^{-3}); 2nd fraction (>98%ee): CD ($CHCl_3$): λ_{max} / nm ($\Delta\varepsilon$ / M^{-1} cm^{-1}, g_{abs}) = 288 (120, 1.0×10^{-3}), 310 (–150, –4.4×10^{-3}), 347 (59, 0.8×10^{-3}), and 374 (–96, –1.5×10^{-3}); CPL ($CHCl_3$): λ_{max} / nm (g_{lum}) = ca. 547 (–7.1×10^{-3}).

3. ^{1}H and ^{13}C NMR spectra

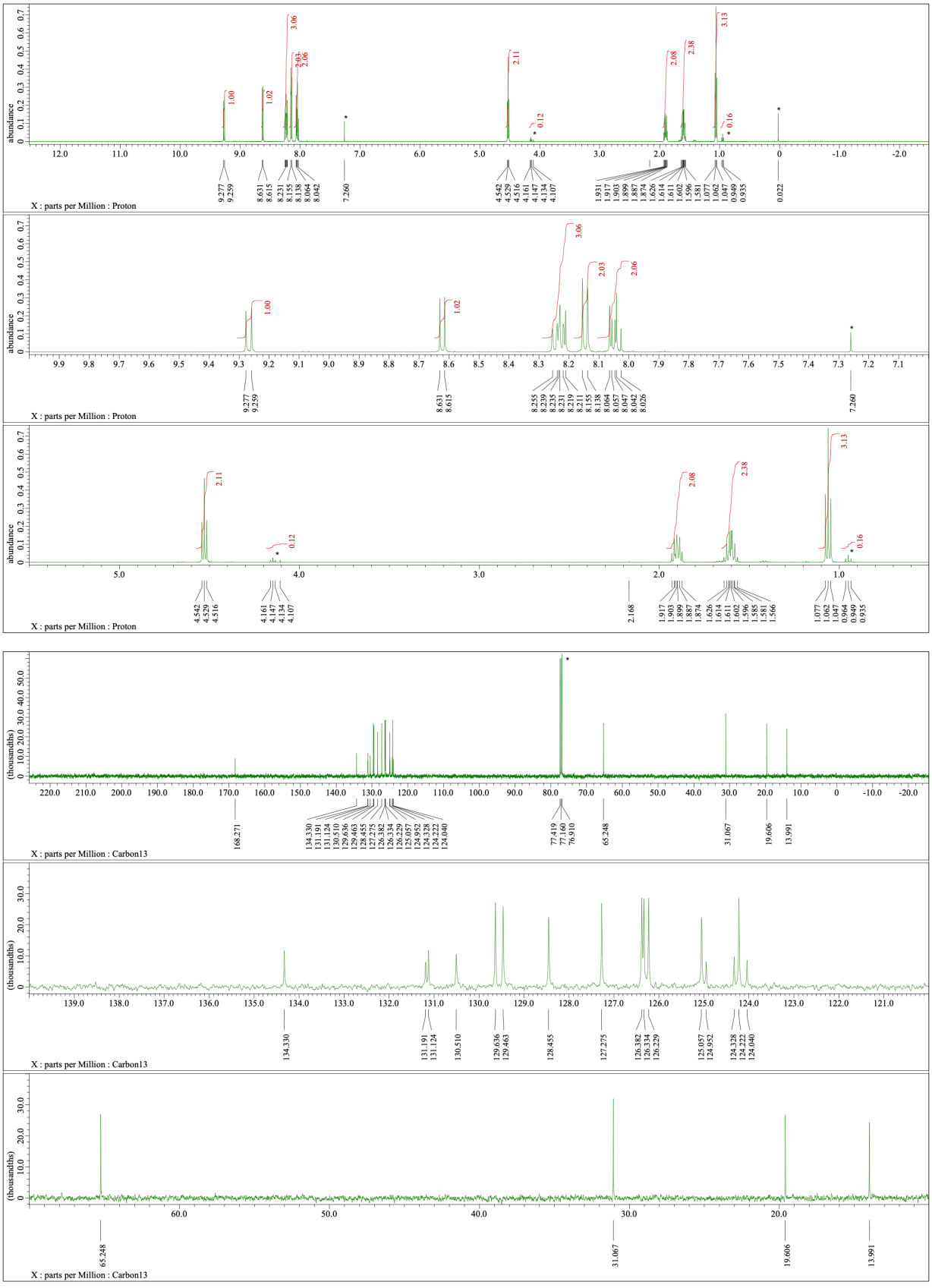

Fig. S3-1. ^{1}H and ^{13}C NMR spectra of **5** in $CDCl_3$ at room temperature. Peaks marked with * are due to residual solvents and impurities.

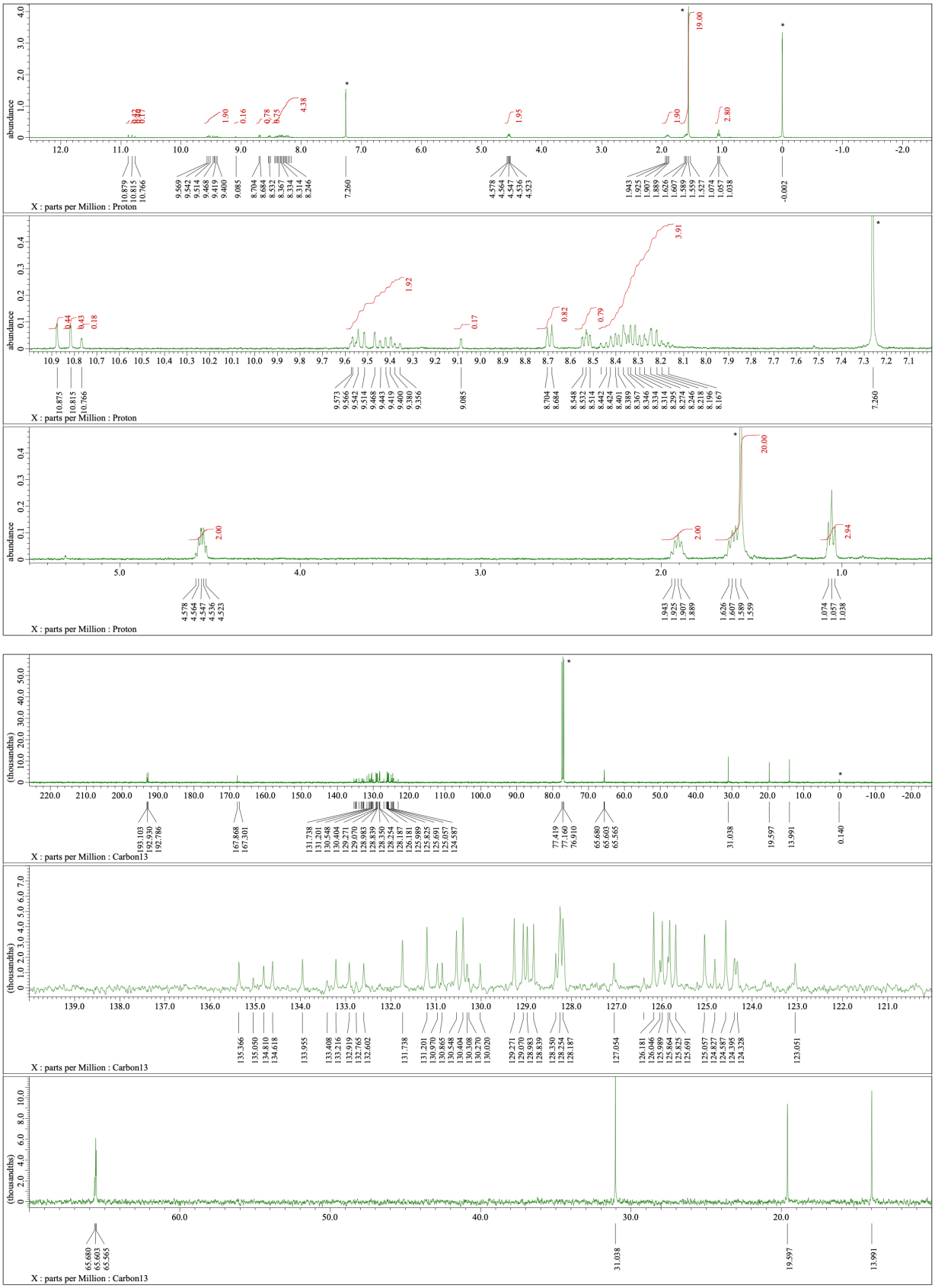

Fig. S3-2. ^{1}H (400 MHz, recorded on a JEOL ECA-400 spectrometer) and ^{13}C NMR spectra of a mixture of **6a**, **6b**, and **6c** in $CDCl_3$ at room temperature. Peaks marked with * are due to residual solvents.

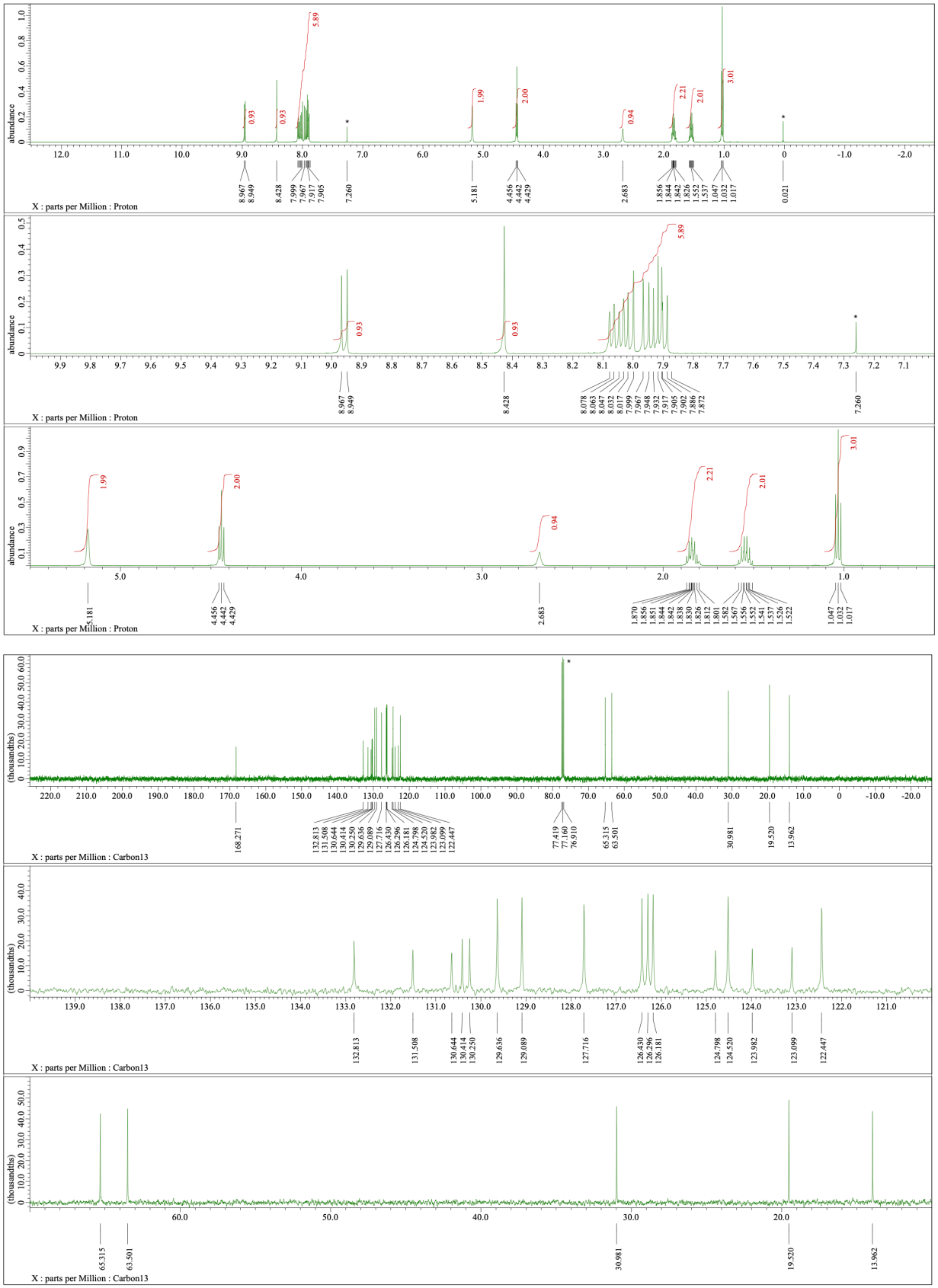

Fig. S3-3. ^{1}H and ^{13}C NMR spectra of **7a** in $CDCl_3$ at room temperature. Peaks marked with * are due to residual solvents.

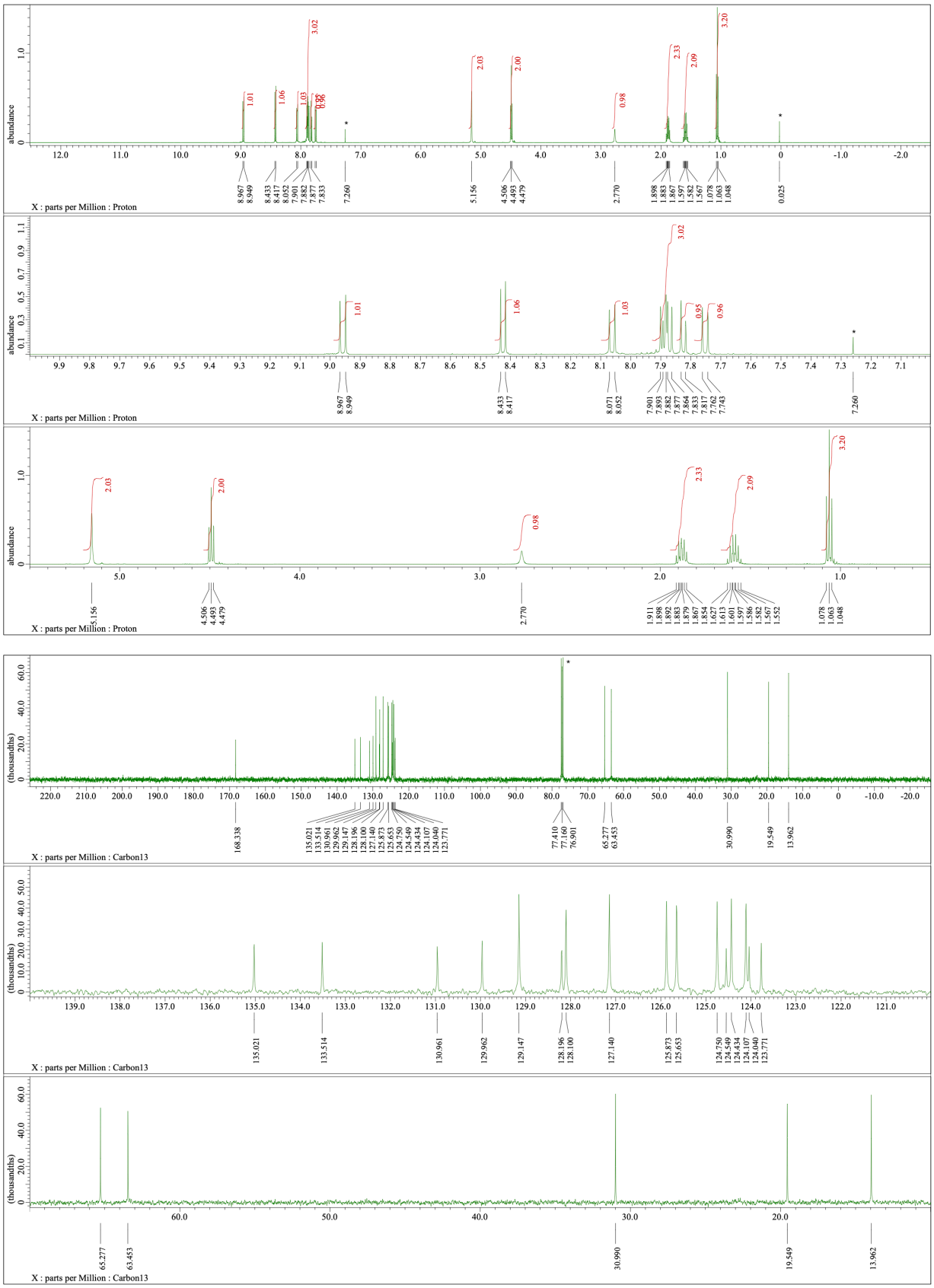

Fig. S3-4. ^{1}H and ^{13}C NMR spectra of **7b** in $CDCl_3$ at room temperature. Peaks marked with * are due to residual solvents.

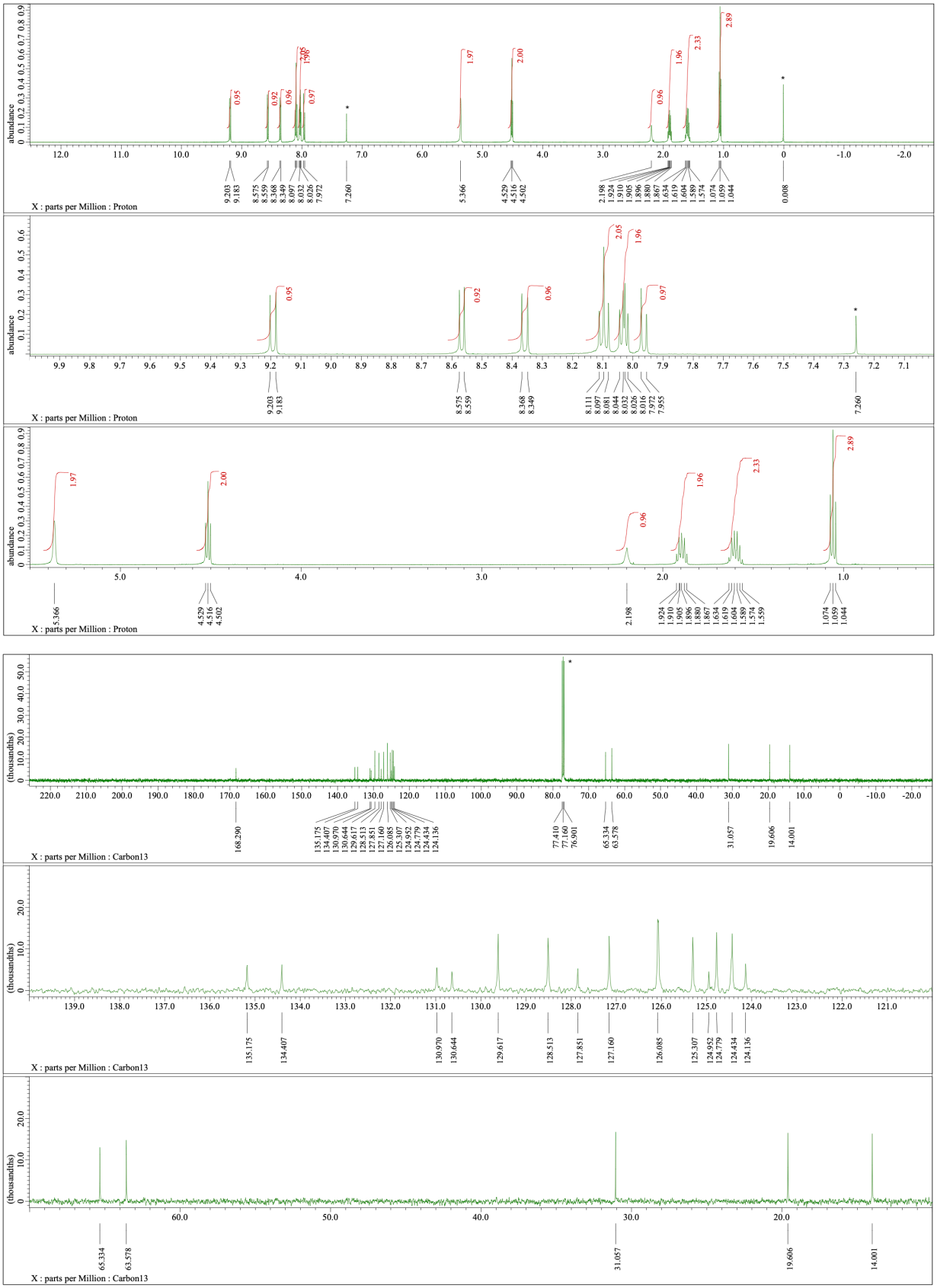

Fig. S3-5. ^{1}H and ^{13}C NMR spectra of **7c** in $CDCl_3$ at room temperature. Peaks marked with * are due to residual solvents.

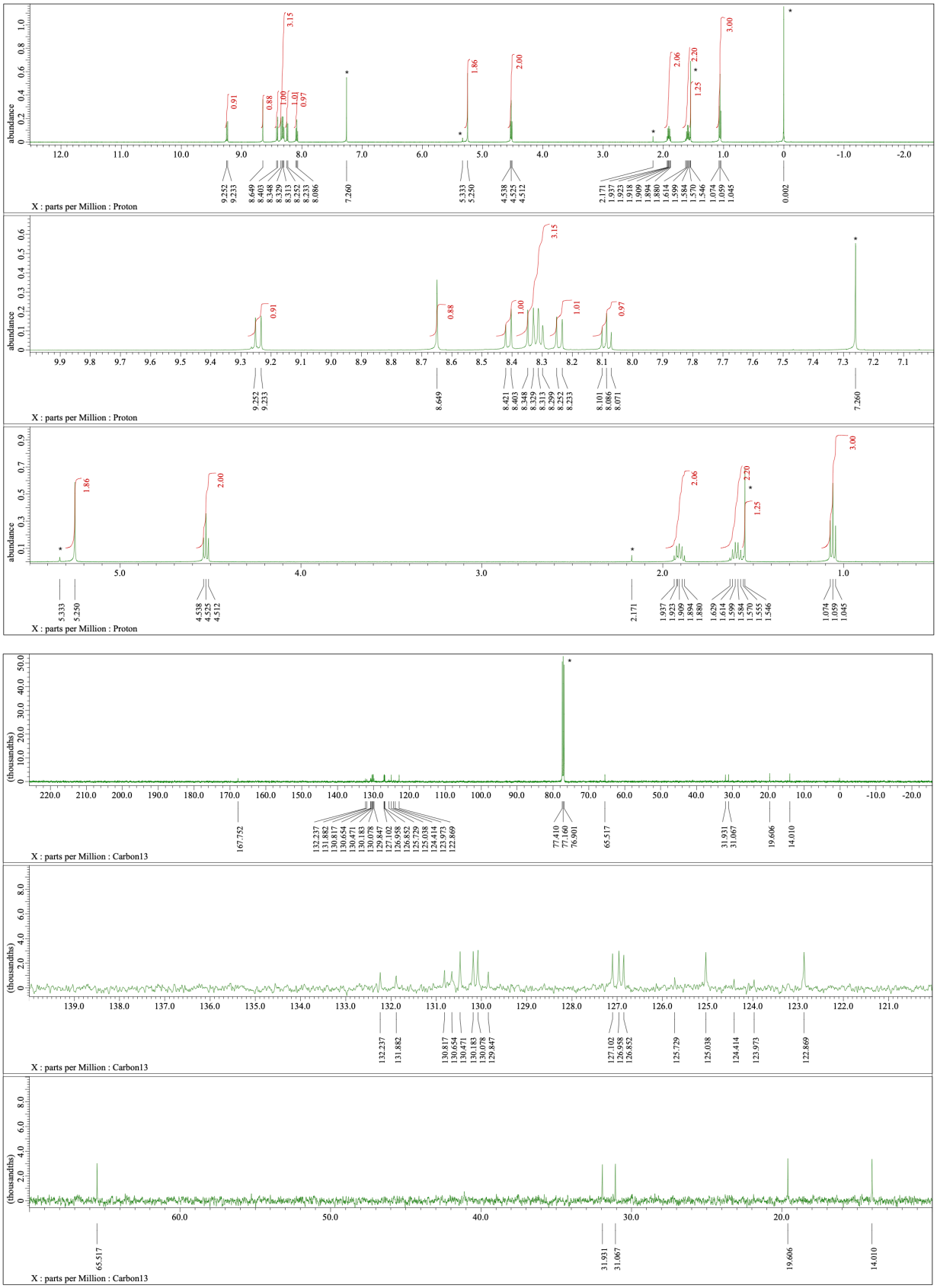

Fig. S3-6. ^{1}H and ^{13}C NMR spectra of **8a** in $CDCl_3$ at room temperature. Peaks marked with * are due to residual solvents.

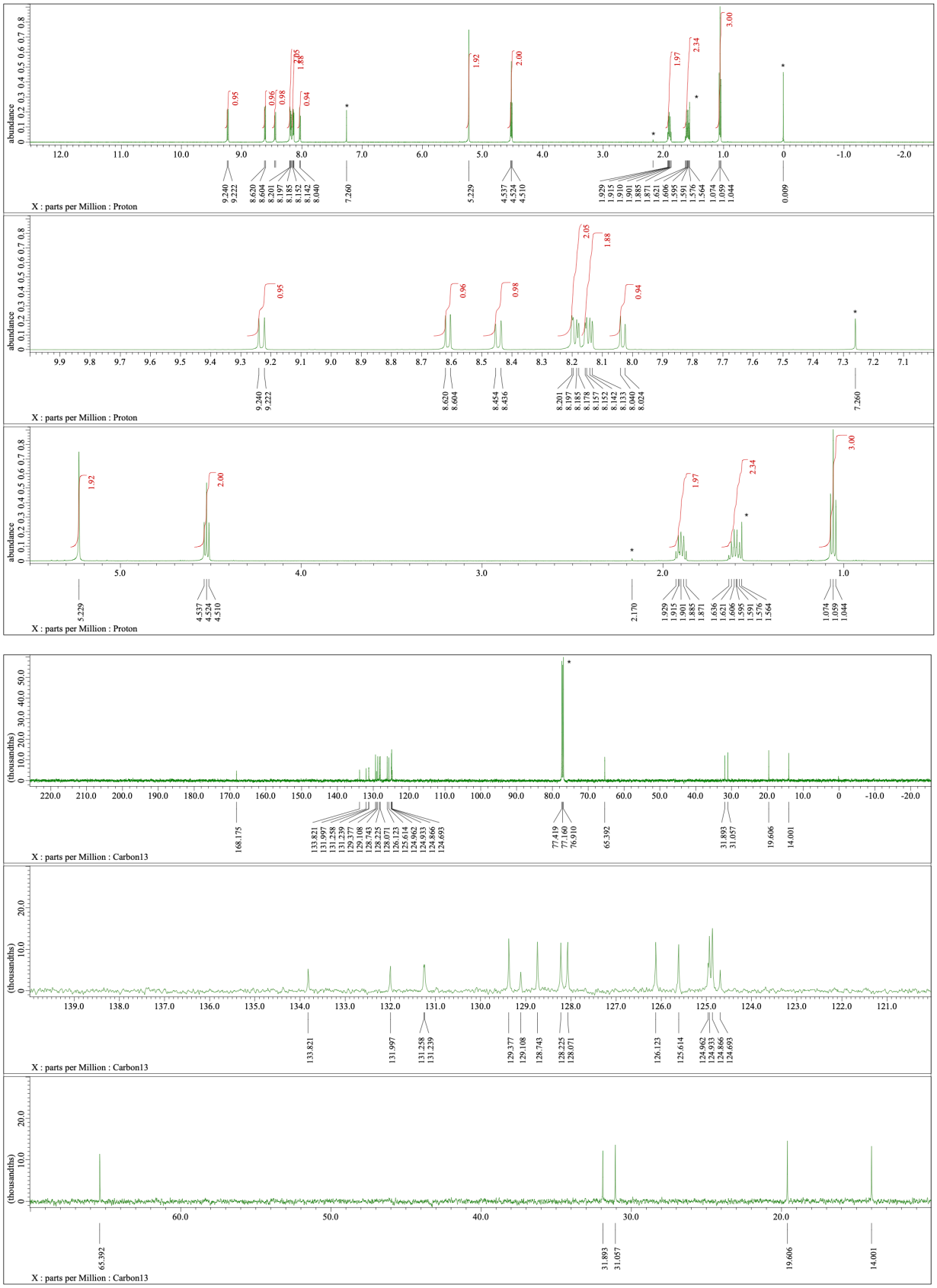

Fig. S3-7. ^{1}H and ^{13}C NMR spectra of **8b** in $CDCl_3$ at room temperature. Peaks marked with * are due to residual solvents.

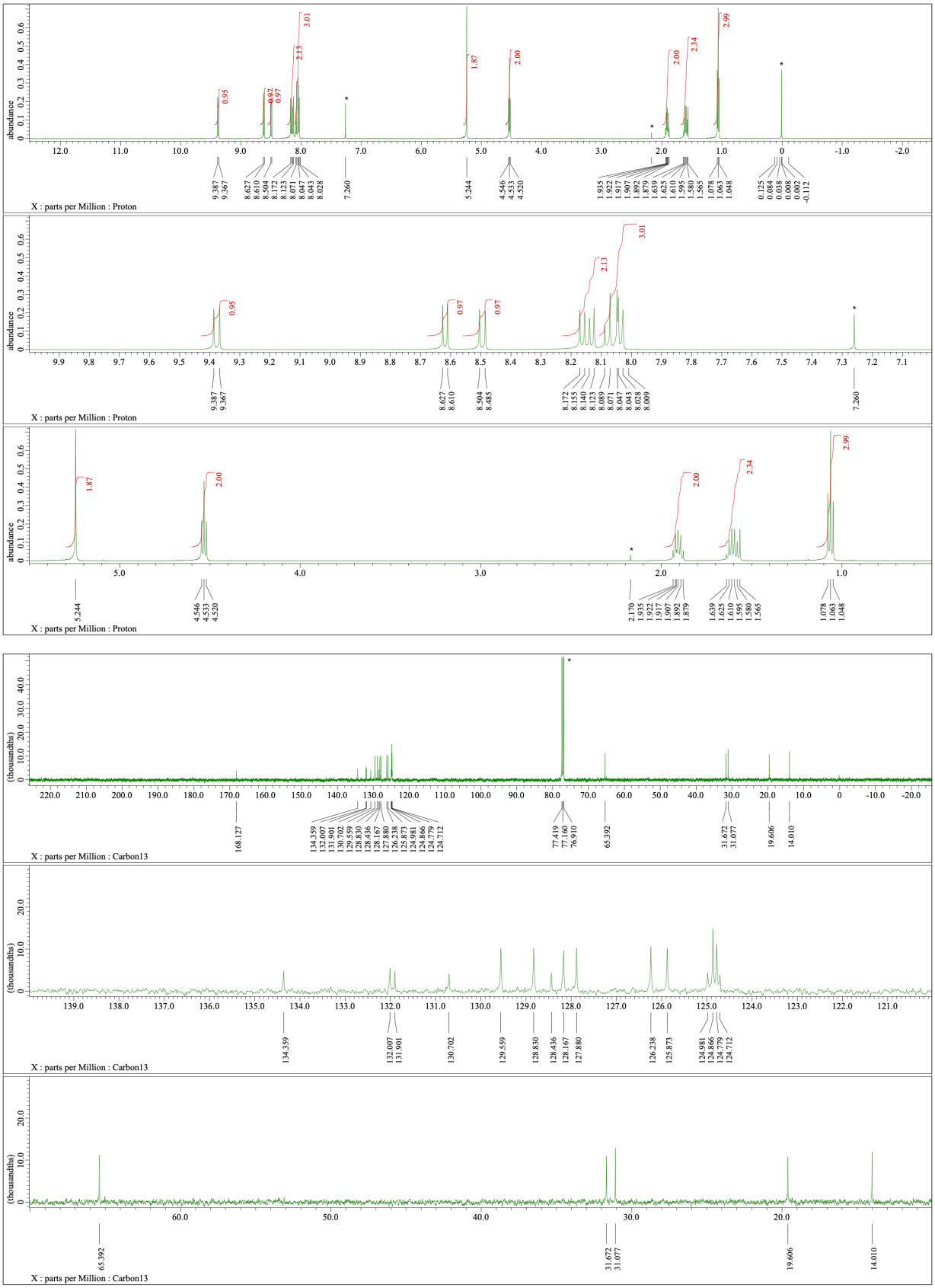

Fig. S3-8. ^{1}H and ^{13}C NMR spectra of **8c** in $CDCl_3$ at room temperature. Peaks marked with * are due to residual solvents.

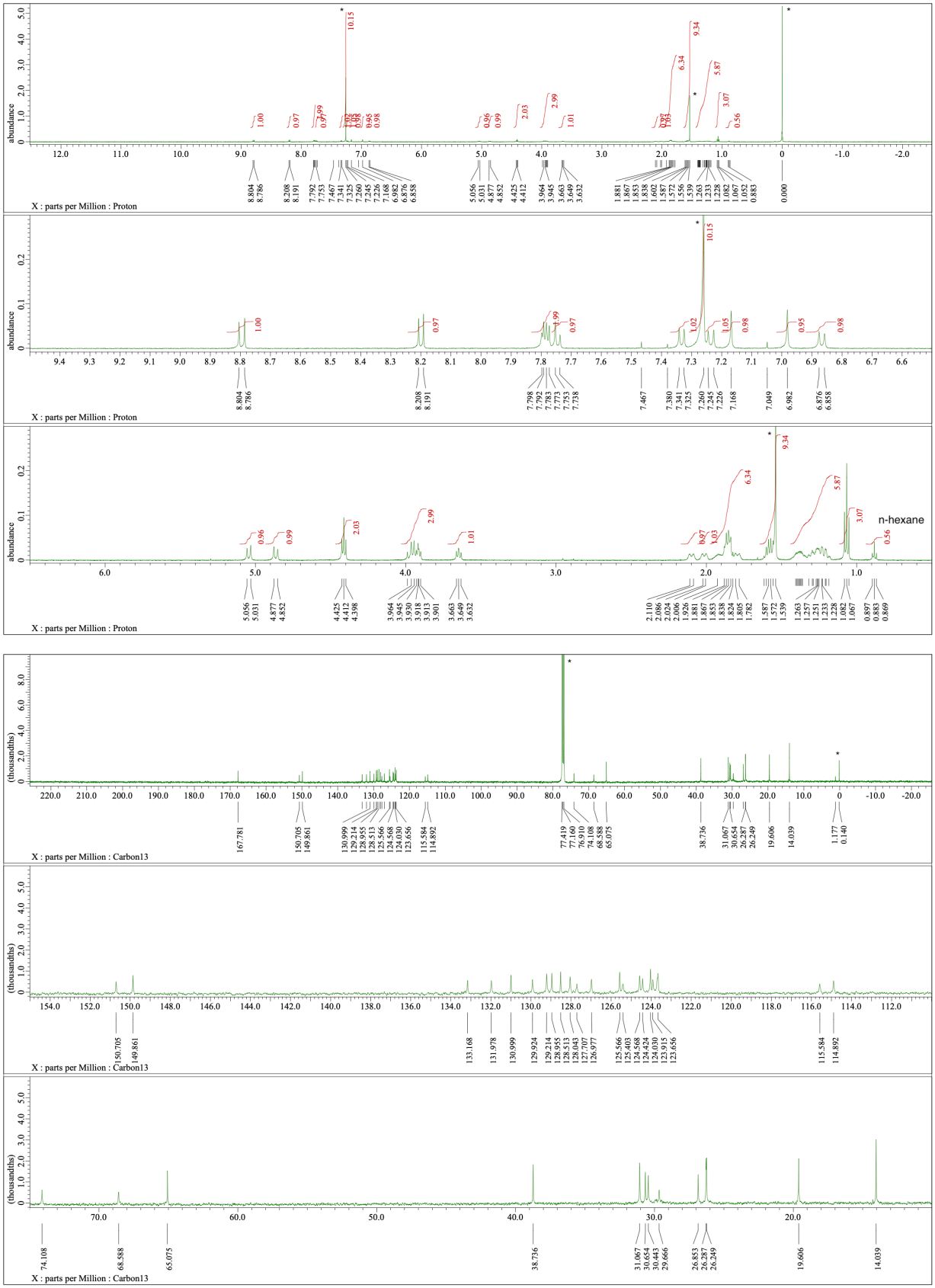

Fig. S3-9. ^{1}H and ^{13}C NMR spectra of **10b** in $CDCl_3$ at room temperature. Peaks marked with * are due to residual solvents.

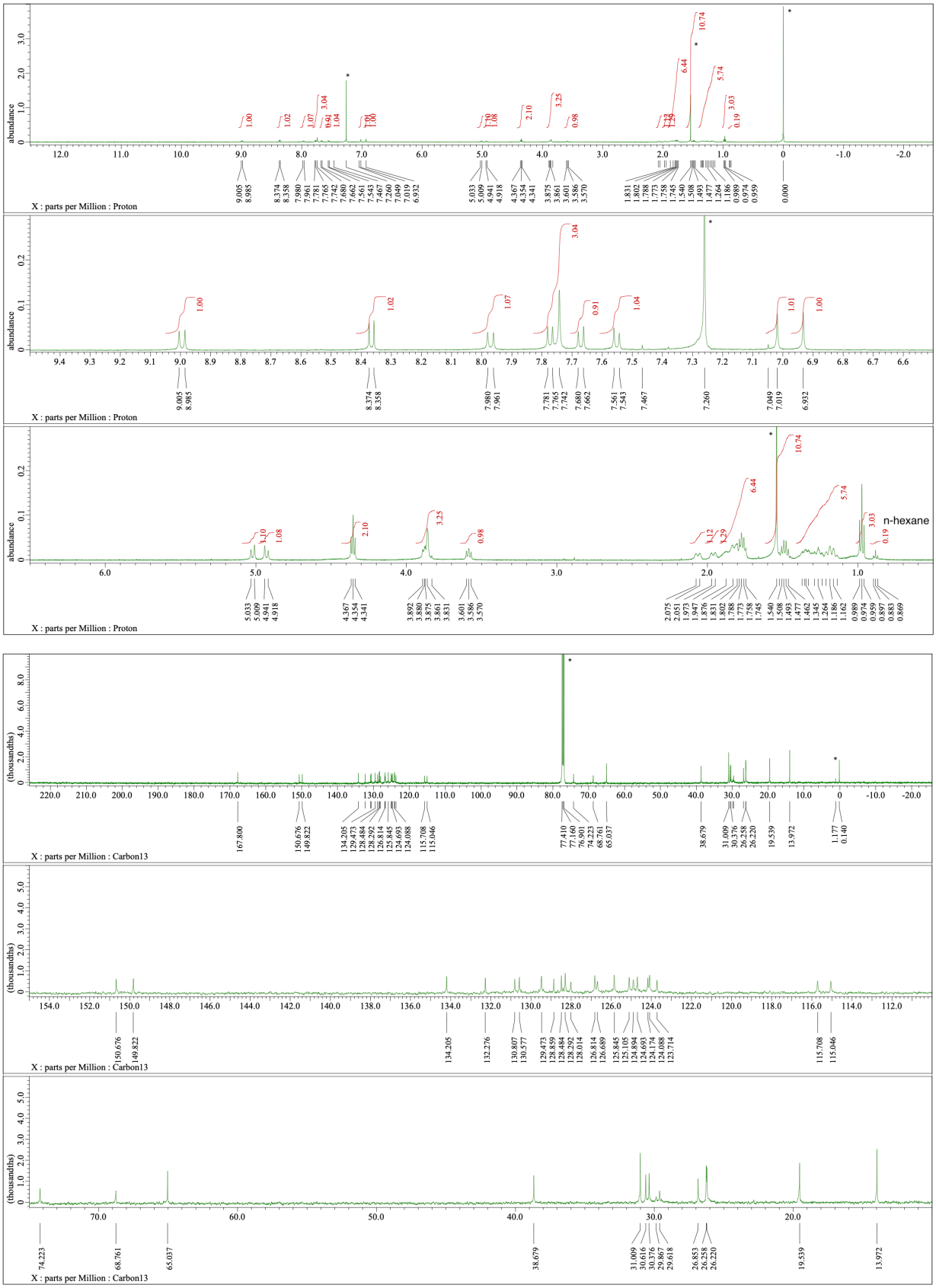

Fig. S3-10. ^{1}H and ^{13}C NMR spectra of **10c** in $CDCl_3$ at room temperature. Peaks marked with * are due to residual solvents.

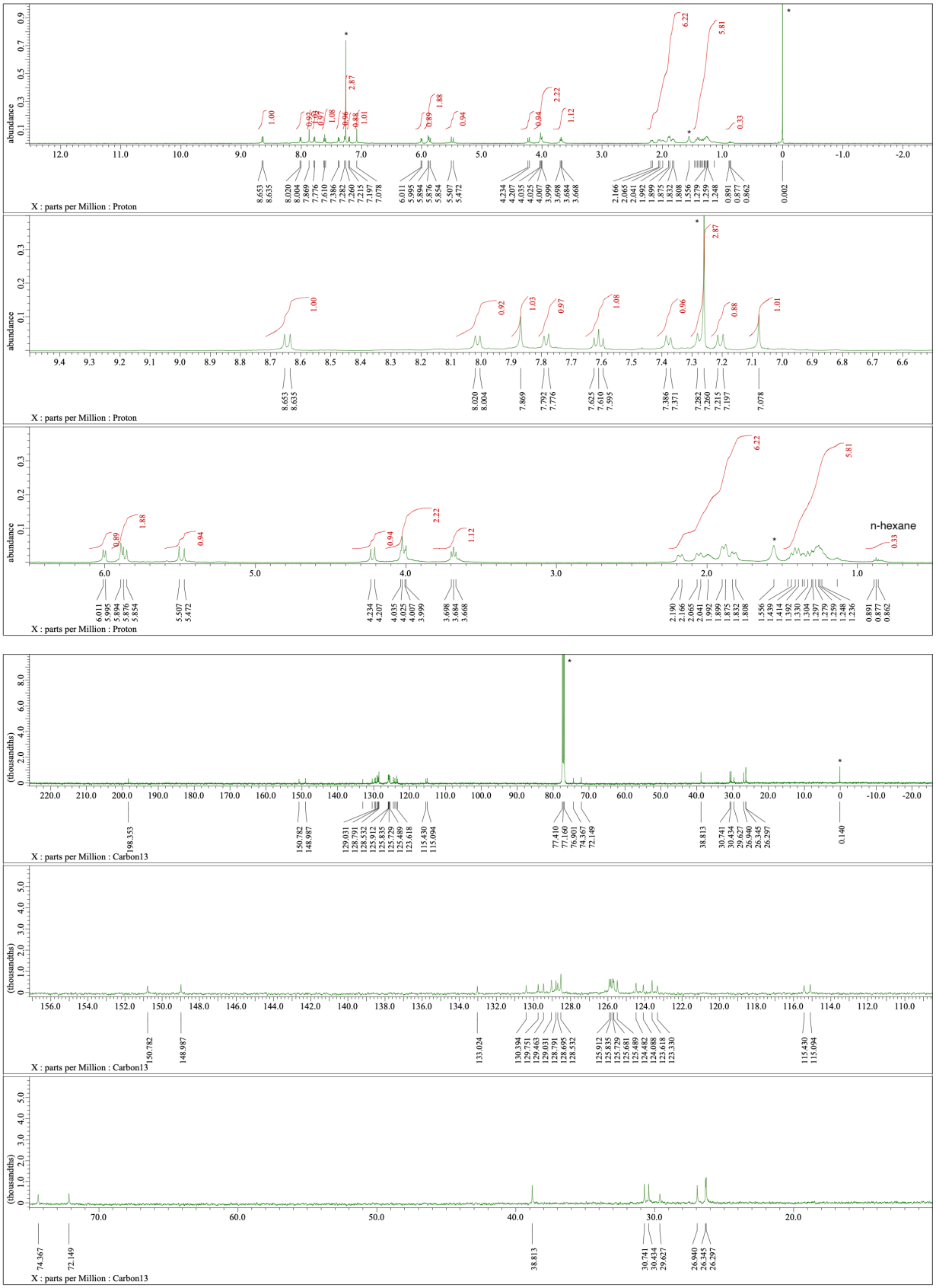

Fig. S3-11. ^{1}H and ^{13}C NMR spectra of **12** in $CDCl_3$ at room temperature. Peaks marked with * are due to residual solvents.

Table S3-1. Summary of 2D NMR correlations of **7b**.

^{1}H peak	COSY*	NOESY	HMQC	HMBC	
				substituent	aromatic
8.96 (d, *J* = 9.0 Hz, 1H)	a	–	124.43	–	129.96, ~125
8.43 (d, *J* = 8.0 Hz, 1H)	b	–	128.10	168.34 (C=O)	133.51, 130.96
8.06 (d, *J* = 9.5 Hz, 1H)	c	5.16 ($\underline{C}H_2OH$)	124.75	–	133.51, ~124
7.91–7.86 (m, 3H)	d	–	125.65	–	135.02, 129.15
	b		124.11	–	~128, ~124
	a		129.15	–	130.96, ~124
8.33 (d, *J* = 8.0 Hz, 1H)	d	5.16 ($\underline{C}H_2OH$)	127.14	63.45 ($\underline{C}H_2OH$)	129.15
7.75 (d, *J* = 9.5 Hz, 1H)	c		125.87		129.15, ~125

*Correlated pairs are shown with alphabets.

Table S3-2. Summary of 2D NMR correlations of **7c**.

^{1}H peak	COSY	NOESY	HMQC	HMBC	
				substituent	aromatic
9.20 (d, *J* = 9.8 Hz, 1H)	a	–	125.31	–	127.85, ~125
8.57 (d, *J* = 8.0 Hz, 1H)	b	–	128.51	168.29 (C=O)	134.41, 130.64
8.36 (d, *J* = 9.8 Hz, 1H)	a	5.37 ($\underline{C}H_2OH$)	124.78	–	130.64, ~124
8.12–8.08 (m, 2H)	c	–	126.09	–	135.18, 129.62, ~124
	b		124.43	–	~127, 124.14
8.05–8.01 (m, 2H)	d	5.37 ($\underline{C}H_2OH$)	129.62	63.58 ($\underline{C}H_2OH$)	134.41, ~124
	c		126.09		130.97, ~127
7.96 (d, *J* = 8.8 Hz, 1H)	d	–	127.16	–	130.97, ~124

*Correlated pairs are shown with alphabets.

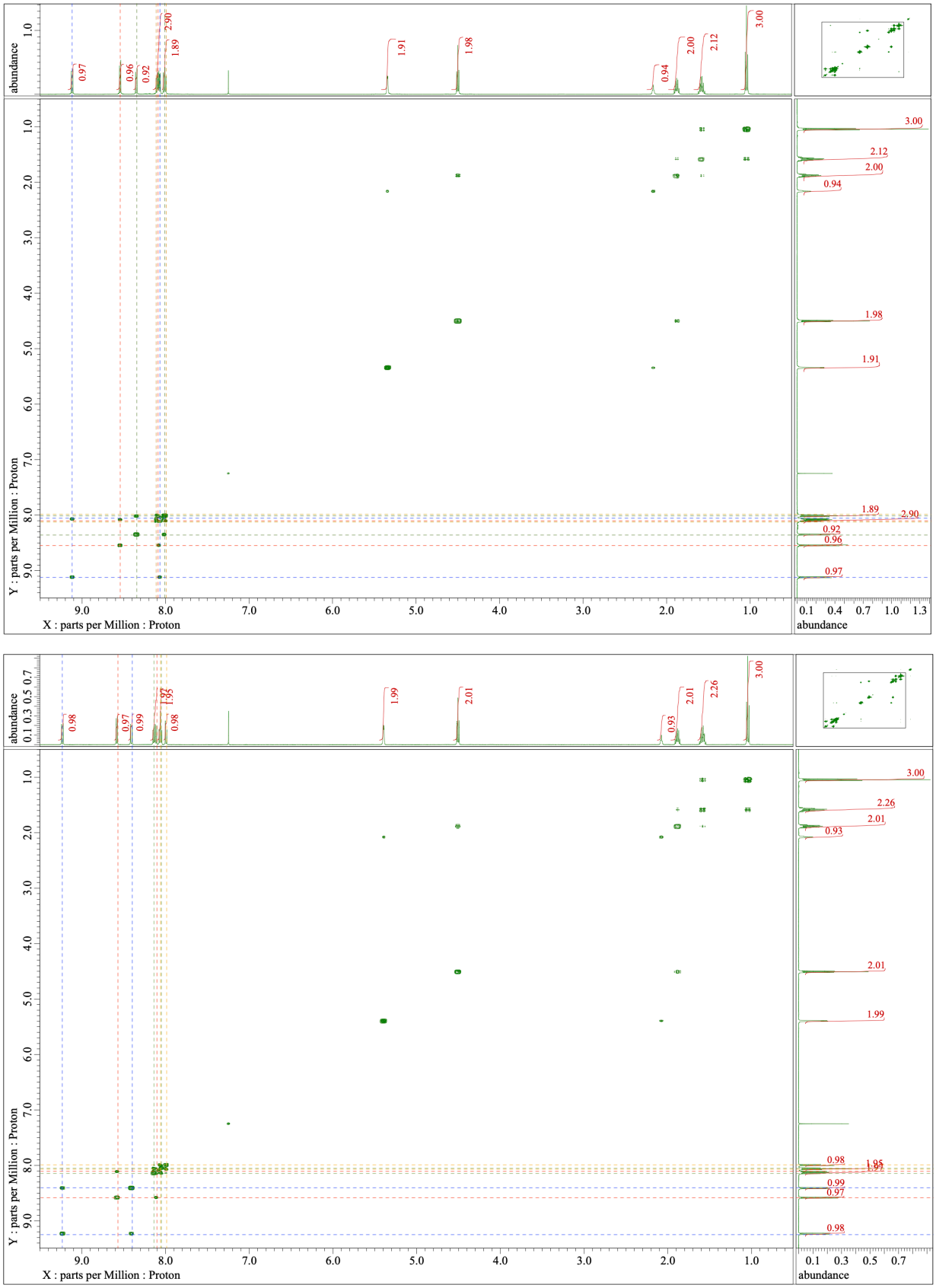

Fig. S3-12. ^{1}H-^{1}H COSY spectra of **7b** (top) and **7c** (bottom) in $CDCl_3$ at room temperature.

Fig. S3-13. ^{1}H-^{1}H NOESY spectra of **7b** (top) and **7c** (bottom) in $CDCl_3$ at room temperature.

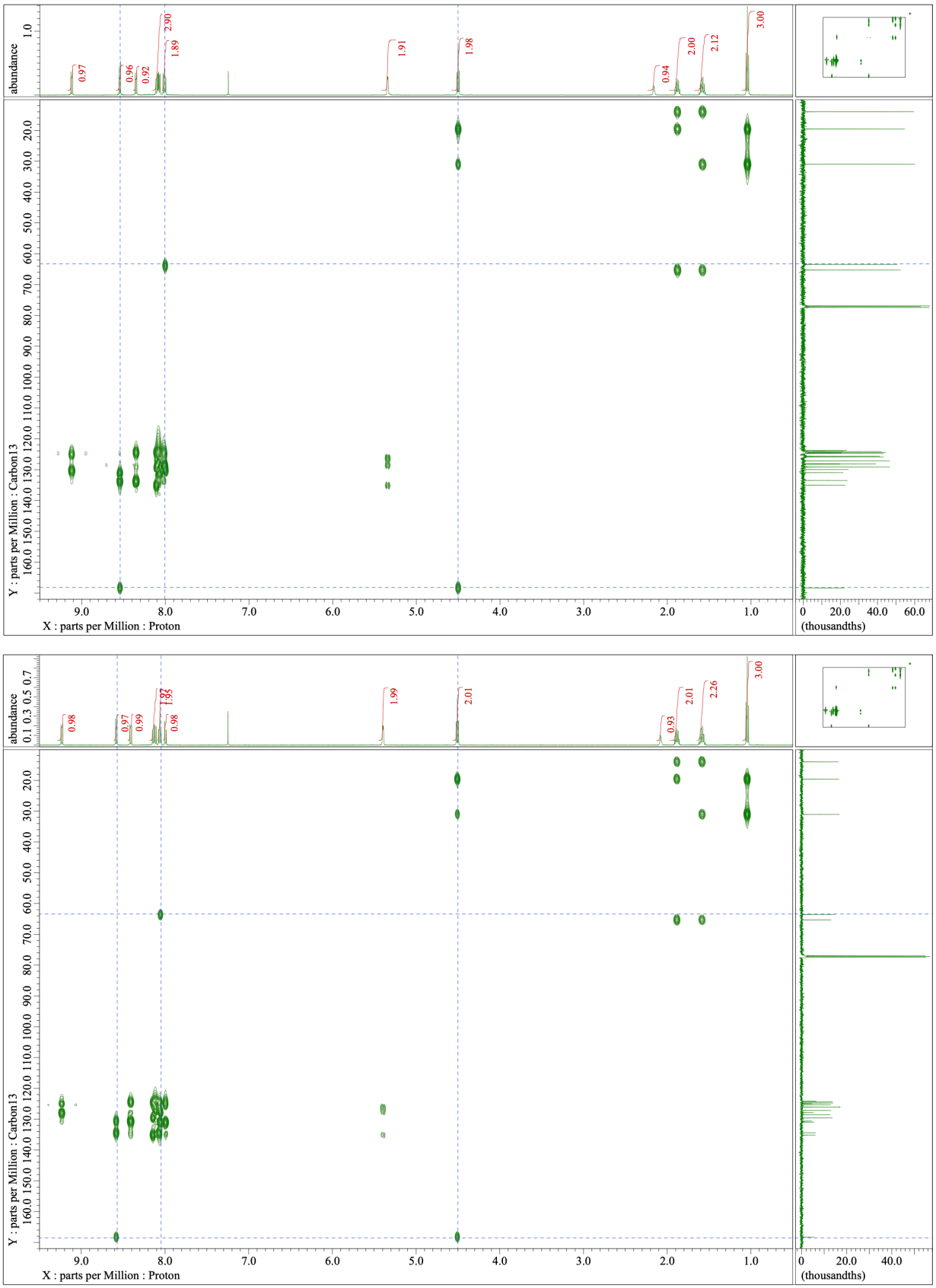

Fig. S3-14. ^{1}H-^{13}C HMBC spectra of **7b** (top) and **7c** (bottom) in $CDCl_3$ at room temperature.

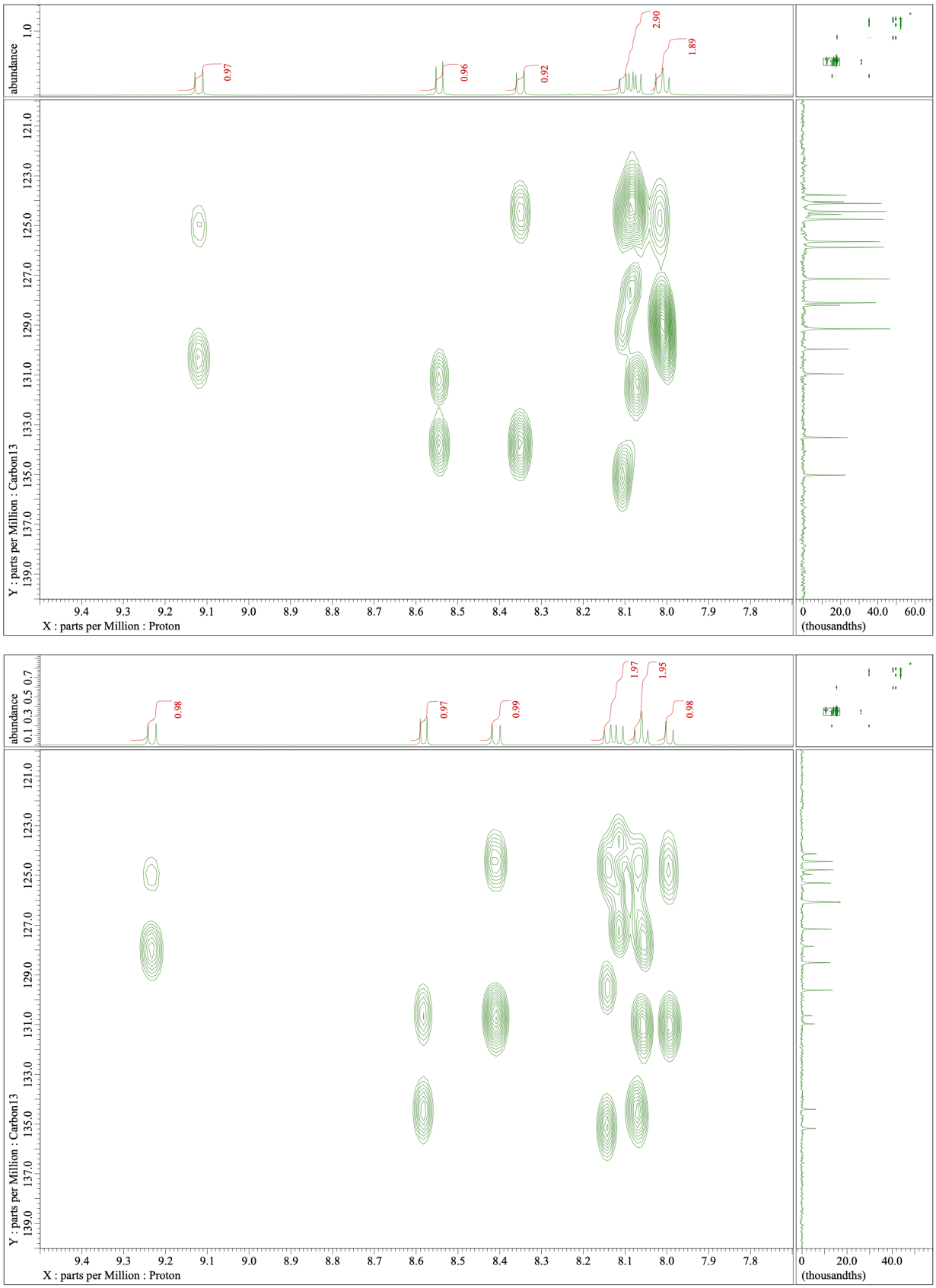

Fig. S3-15. Selected region of ^{1}H-^{13}C HMBC spectra of **7b** (top) and **7c** (bottom) in $CDCl_3$ at room temperature.

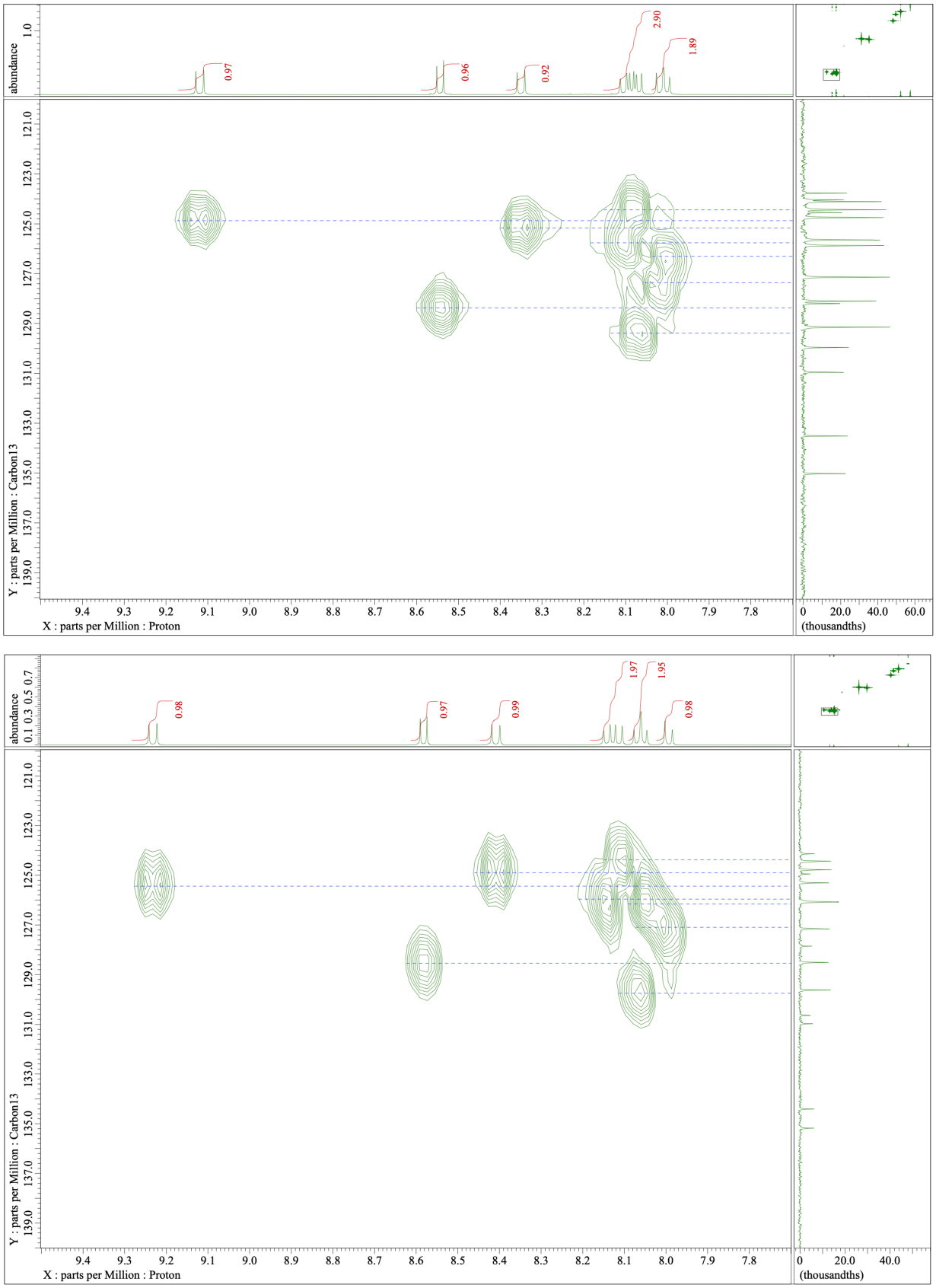

Fig. S3-16. Selected region of ^{1}H-^{13}C HMQC spectra of **7b** (top) and **7c** (bottom) in $CDCl_3$ at room temperature.

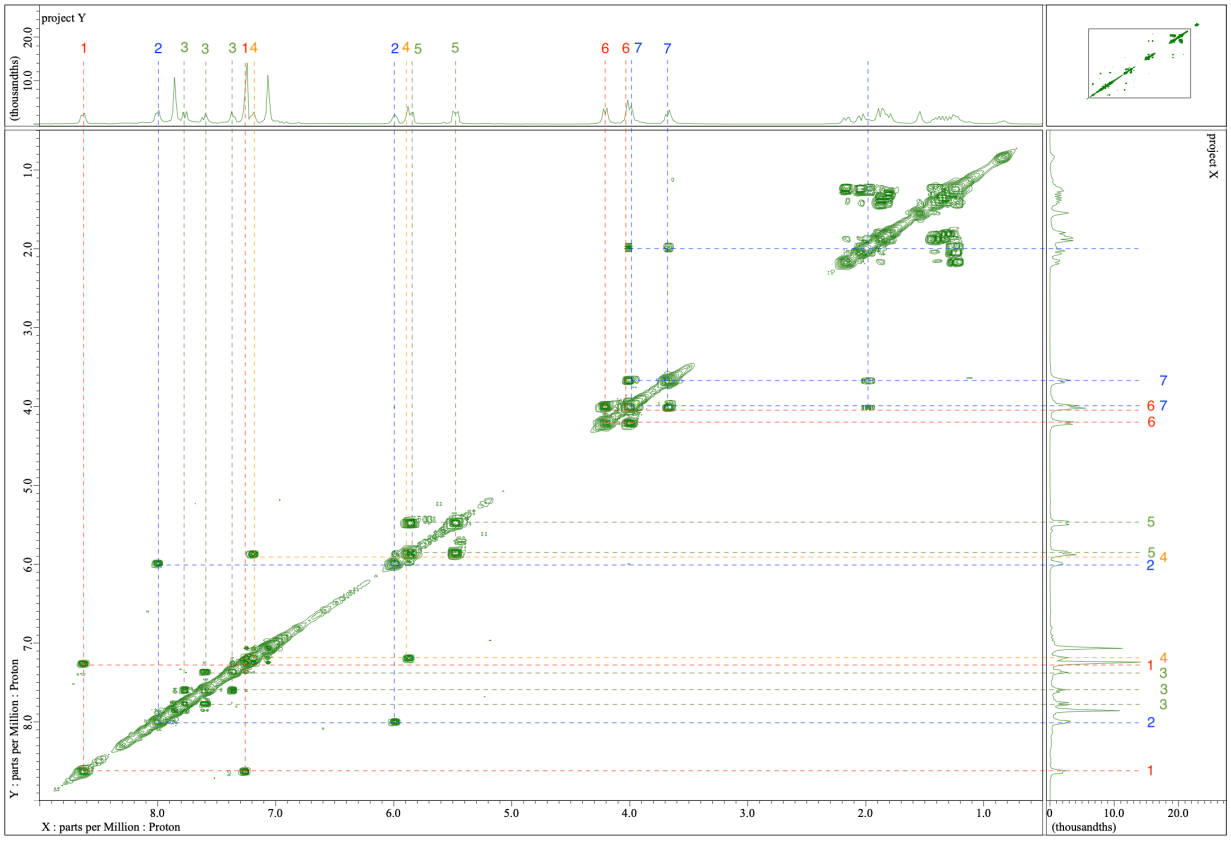

Fig. S3-17. ^{1}H-^{1}H COSY spectrum of **12** in $CDCl_3$ at room temperature.

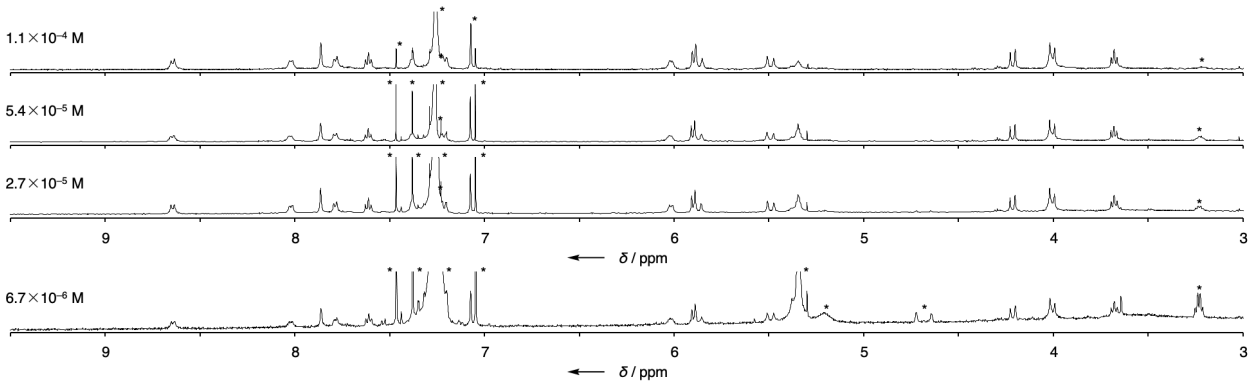

Fig. S3-18. Selected region of concentration-dependent ^{1}H NMR spectra of **12** in $CDCl_3$ at room temperature. The concentration of 6.7×10^{-6} M roughly corresponded to that used for fluorescence and CPL measurement. Spectra were also acquired in higher concentrations, but no concentration dependence was observed. Peaks marked with * are due to residual solvents and impurities.

4. High-resolution APCI-FT-MS and MALDI-TOF-MS

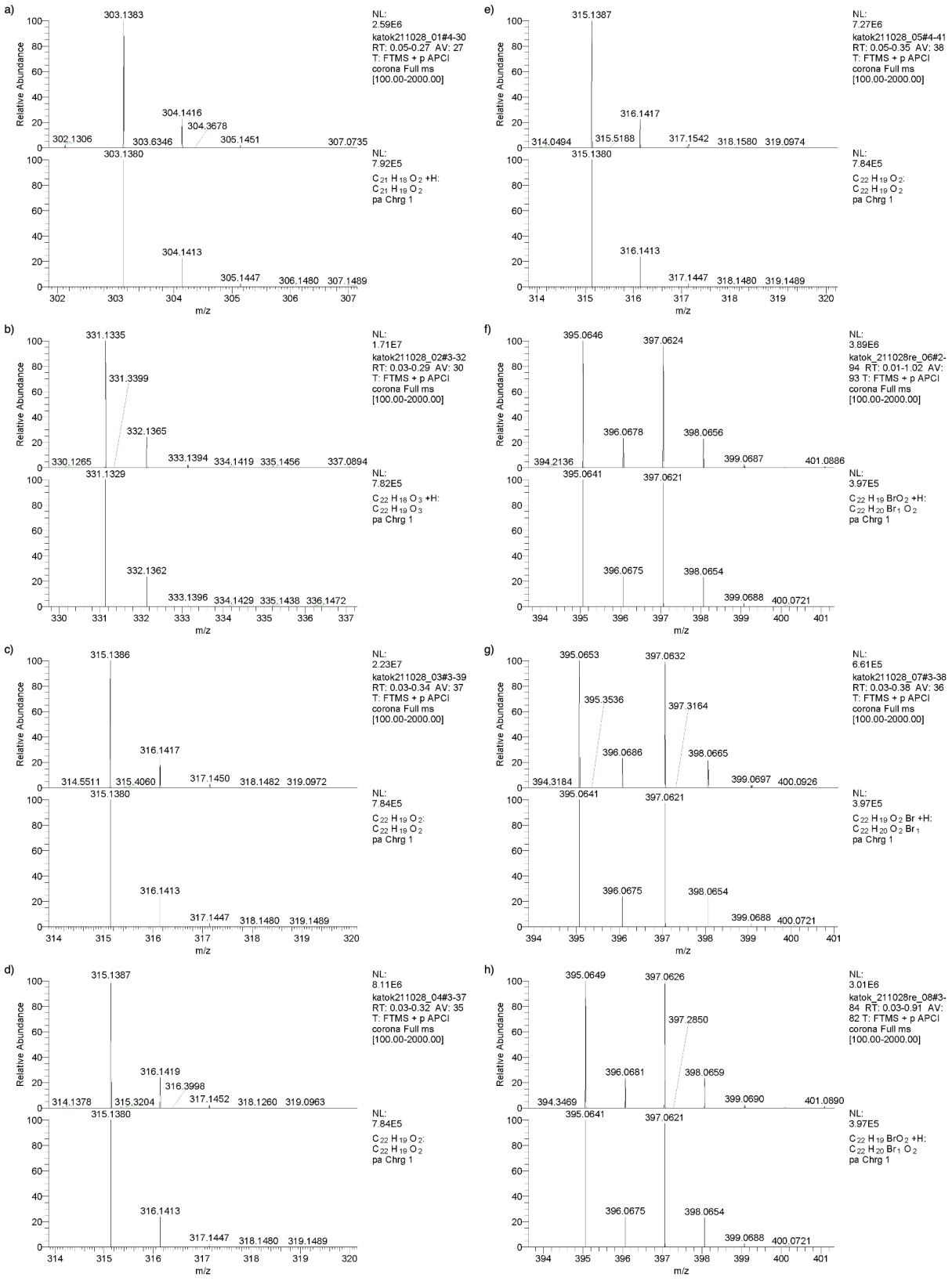

Fig. S4-1. Observed (top) and simulated (bottom) high-resolution APCI-FT-MS results of a) **5**, b) a mixture of **6a**, **6b**, and **6c**, c) **7a**, d) **7b**, e) **7c**, f) **8a**, g) **8b**, and h) **8c**.

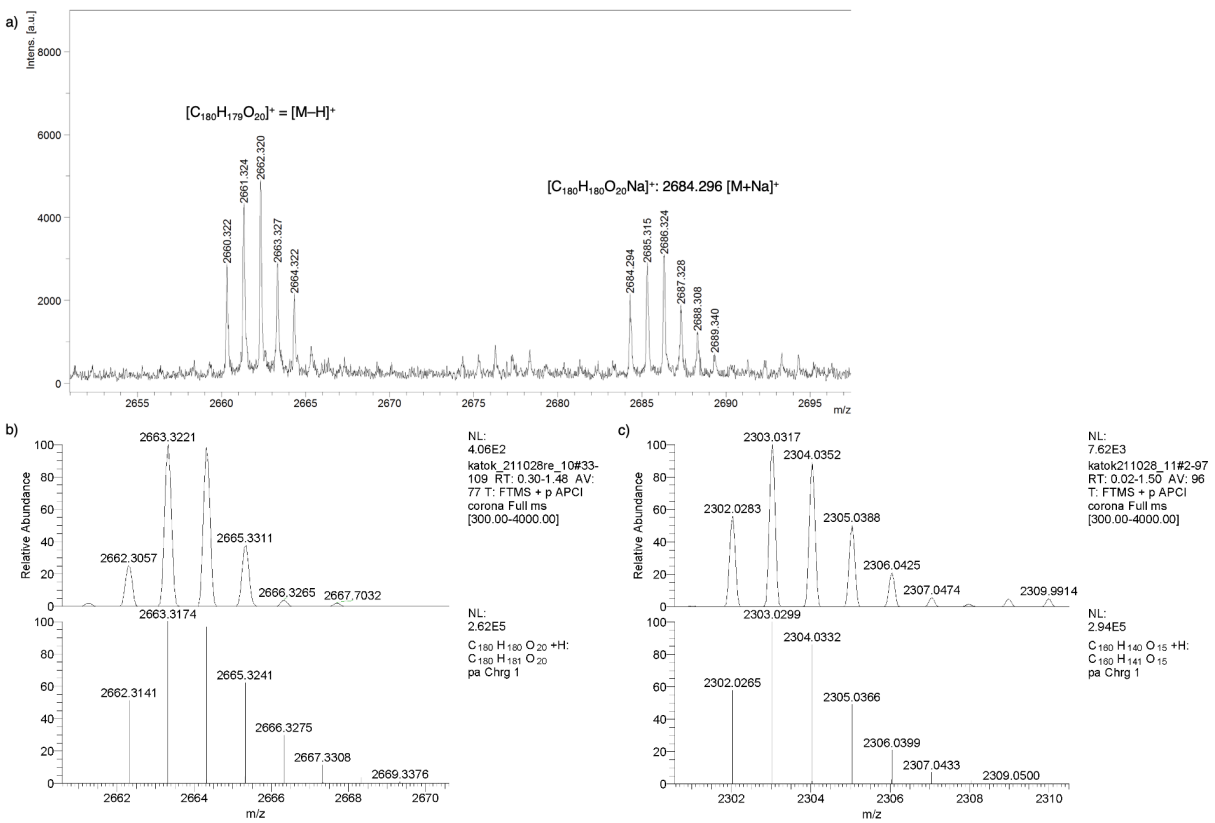

Fig. S4-2. a) Observed MALDI-TOF-MS result of **10b**. Observed (top) and simulated (bottom) high-resolution APCI-FT-MS results of b) **10c** and c) **12**.

5. UV/vis absorption and fluorescence spectra

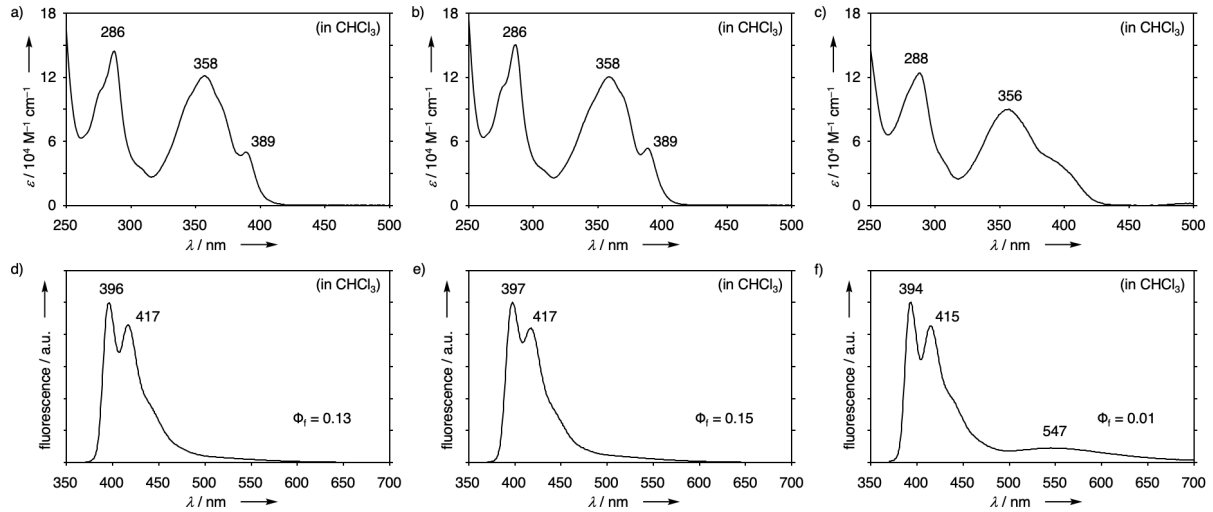

Fig. S5-1. UV/vis absorption spectra of a) **10b**, b) **10c**, and c) **12** in $CHCl_3$. Fluorescence spectra of d) **10b** (3.1×10^{-6} M), e) **10c** (2.7×10^{-6} M), and f) **12** (4.4×10^{-6} M) in $CHCl_3$. Excitation wavelength was set at 350 nm.

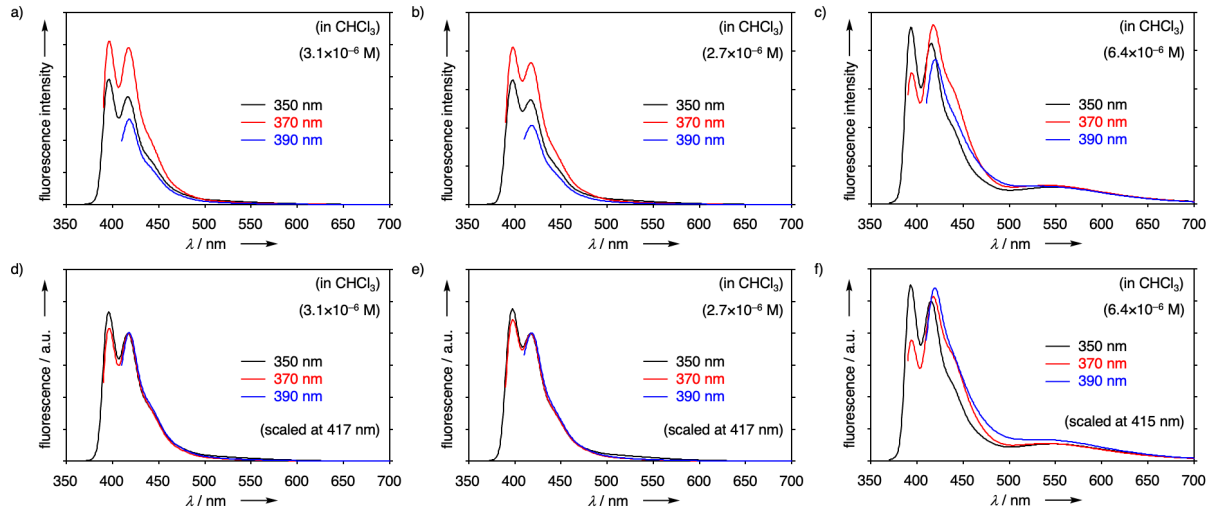

Fig. S5-2. Fluorescence spectra of a) **10b**, b) **10c**, and c) **12** with different excitation wavelengths (black: 350 nm; red: 370 nm; blue: 390 nm) in $CHCl_3$. The spectra were scaled by the intensities at 417 nm for d) **10b** and e) **10c**, and 415 nm for f) **12**. The red shifts in **12** could not be ascribed to self-absorption because of absence of absorption over 440 nm.

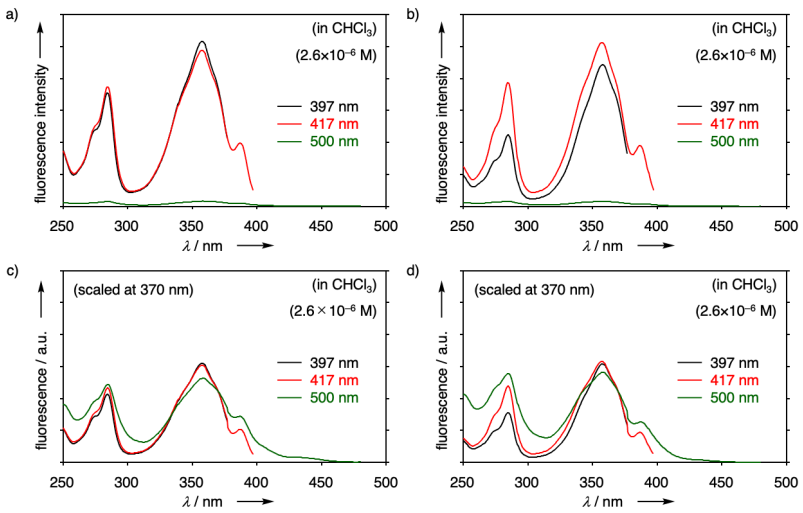

Fig. S5-3. Excitation spectra of a) **10b** and b) **10c** with different detection wavelengths (black: 397 nm; red: 417 nm; green: 500 nm) in $CHCl_3$. The spectra of c) **10b** and d) **10c** were scaled by the intensities at 370 nm.

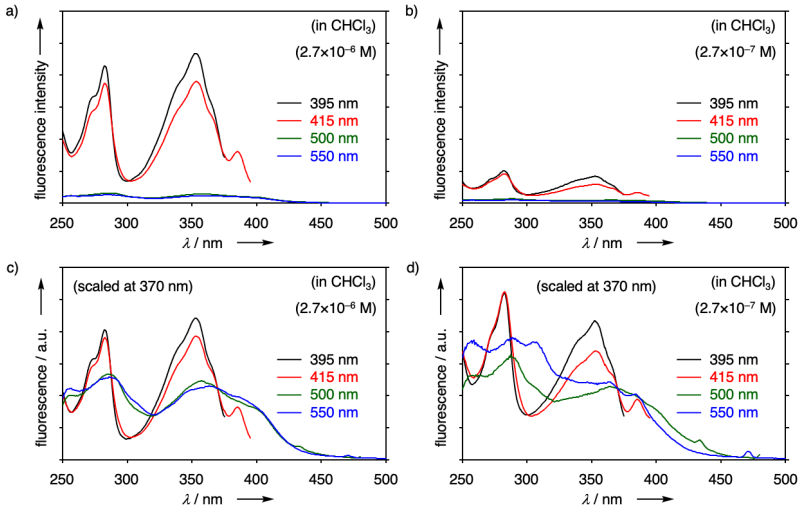

Fig. S5-4. Excitation spectra of **12** with different detection wavelengths (black: 397 nm; red: 417 nm; green: 500 nm; blue: 550 nm) in $CHCl_3$. The spectra were recorded at a) 2.7×10^{-6} M and b) 2.7×10^{-7} M, which were scaled by the intensities at 370 nm in figures c) and d) respectively. To exclude possible contributions of impurities, racemic **12** of NMR quality was purified with a chiral HPLC system. The fluorescence spectra of these samples were confirmed to be identical to each other.

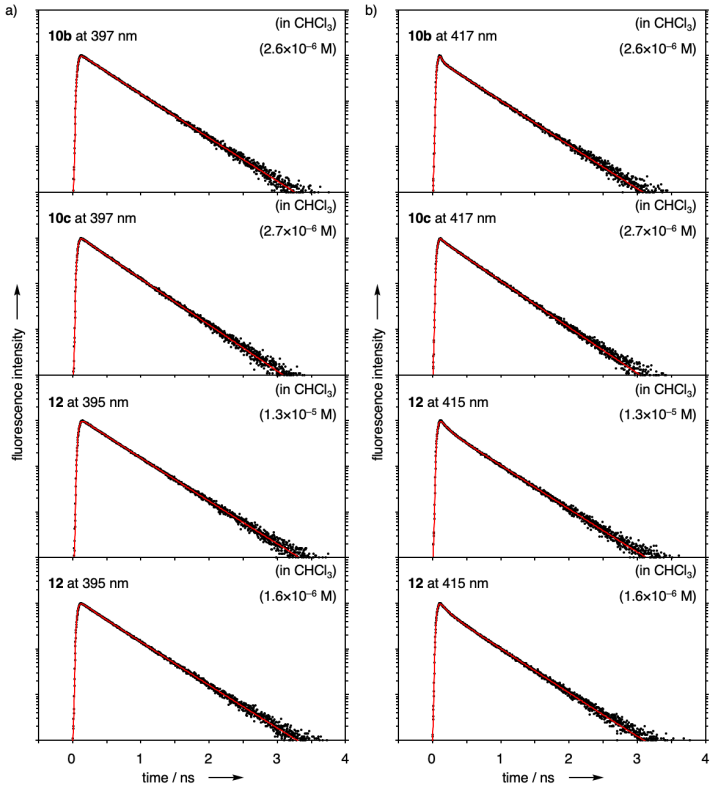

Fig. S5-5. Emission lifetime measurement of **10b** (top), **10c** (2nd), and **12** (3rd and bottom) with detection wavelengths at a) 397 or 395 nm and b) 417 or 415 nm in $CHCl_3$ (excitation wavelength was set at 369 nm).

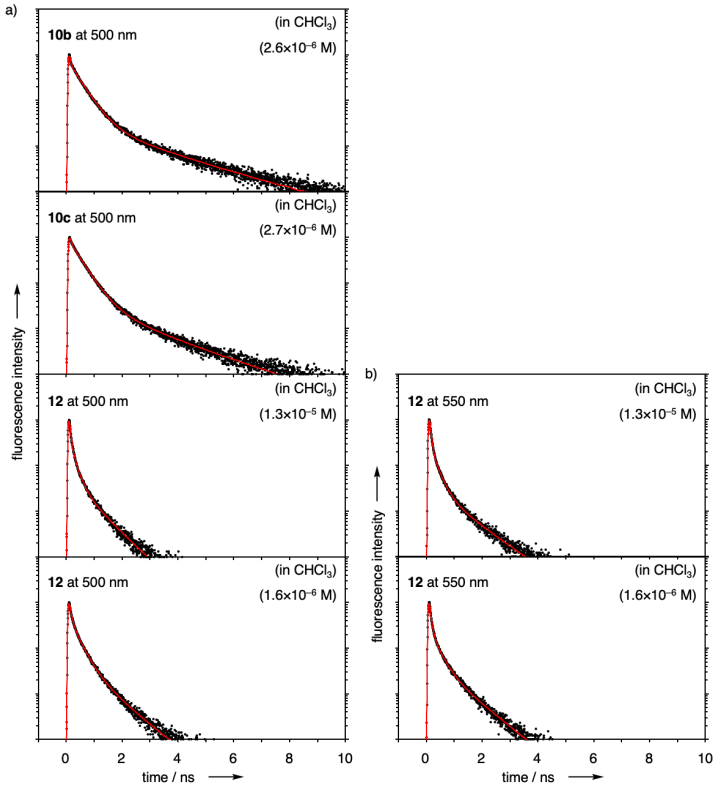

Fig. S5-6. Emission lifetime measurement of **10b** (top), **10c** (2nd), and **12** (3rd and bottom) with detection wavelengths at a) 397 or 395 nm and b) 417 or 415 nm in $CHCl_3$ (excitation wavelength was set at 369 nm).

Table S5-1. Fitting parameters for emission lifetime measurement.

compound	397/395 nm			417/415 nm			500 nm			550 nm		
concentration	τ [ns]	RA[a]	χ^2	τ [ns]	RA[a]	χ^2	τ [ns]	RA[a]	χ^2	τ [ns]	RA[a]	χ^2
10b	2.2	5.0	1.23	0.30	9.0	1.25	0.30	11.0				
2.6×10⁻⁶ M	4.6	95.0		4.5	91.0		4.2	69.3	1.18	–	–	–
							22.3	19.7				
10c	1.0	2.5	1.24	0.45	3.9	1.16	0.43	6.4				
2.7×10⁻⁶ M	4.3	97.5		4.3	96.1		4.2	76.1	1.17	–	–	–
							19.2	17.5				
12	2.3	3.8	1.28	0.89	12.2	1.21	0.36	44.4		0.47	48.0	
1.3×10⁻⁵ M	4.6	96.2		4.5	87.8		1.8	35.3	1.38	2.3	34.6	1.28
							7.0	20.3		9.7	17.4	
12	1.7	3.4	1.24	0.96	12.0	1.16	0.52	26.8		0.48	42.6	
1.6×10⁻⁶ M	4.6	96.6		4.5	88.0		2.9	52.5	1.31	2.6	34.8	1.26
							8.5	20.7		8.7	22.6	

[a]relative amplitude in percentage.

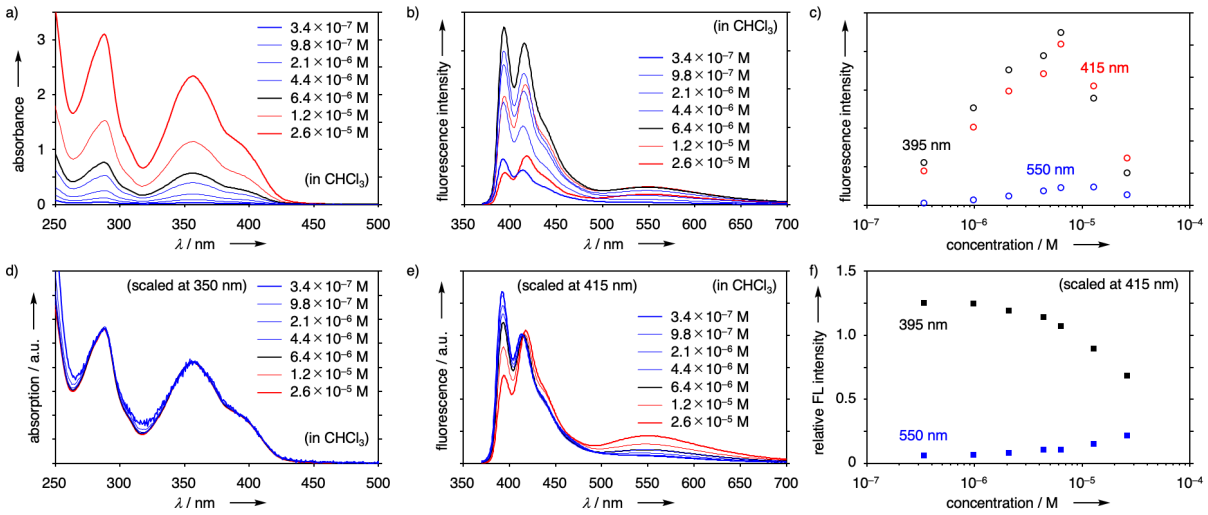

Fig. S5-7. Concentration-dependent a) UV/vis absorption and b) fluorescence spectra (excitation wavelength was set at 350 nm) and c) fluorescence intensity plot (black: 395 nm; red: 417 or 415 nm; blue: 550 nm) of **12** in $CHCl_3$ in the range of 3.4×10⁻⁷ to 2.5×10⁻⁵ M. The spectra were scaled by the intensities at d) 350 nm and 415 nm. f) Relative fluorescence intensity plot of peaks at 395 nm (black) and 550 nm (blue) compared with that at 415 nm. Different from concentration-dependent fluorescence properties, UV/vis absorption followed Lambert–Beer law (small deviation at around 317 nm in 3.4×10⁻⁷ M solution was due to small absorbance values, which amplified errors in baseline by scaling).

6. HPLC charts and chiroptical measurement

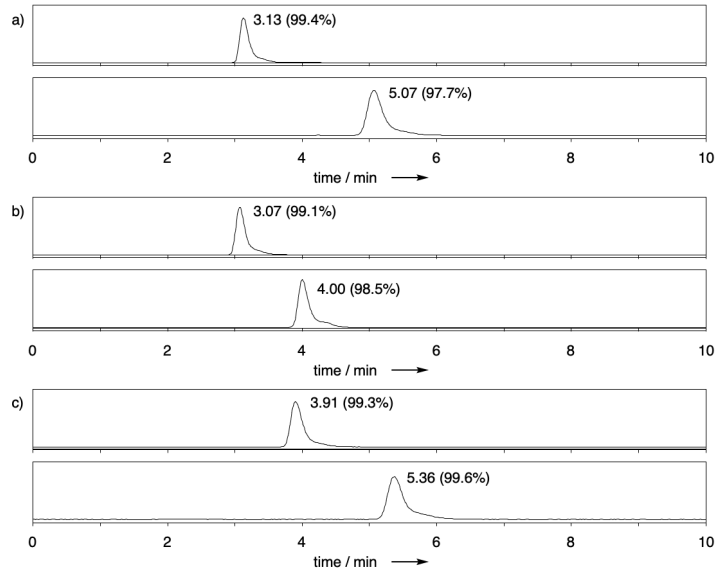

Fig. S6-1. HPLC charts of enantiopure fractions a) **10b**, b) **10c**, and c) **12** recorded as absorption of 350-nm light (top: 1st fractions; bottom: 2nd fractions). Conditions: CHIRALPAK IA (ϕ = 4.6 mm, l = 250 mm) column, room temperature, flow rate = 1.0 mL/min, eluent = CH_2Cl_2/*n*-hexane = 50/50. Retention time [min] of each peak is also shown along with percentage of the peak area.

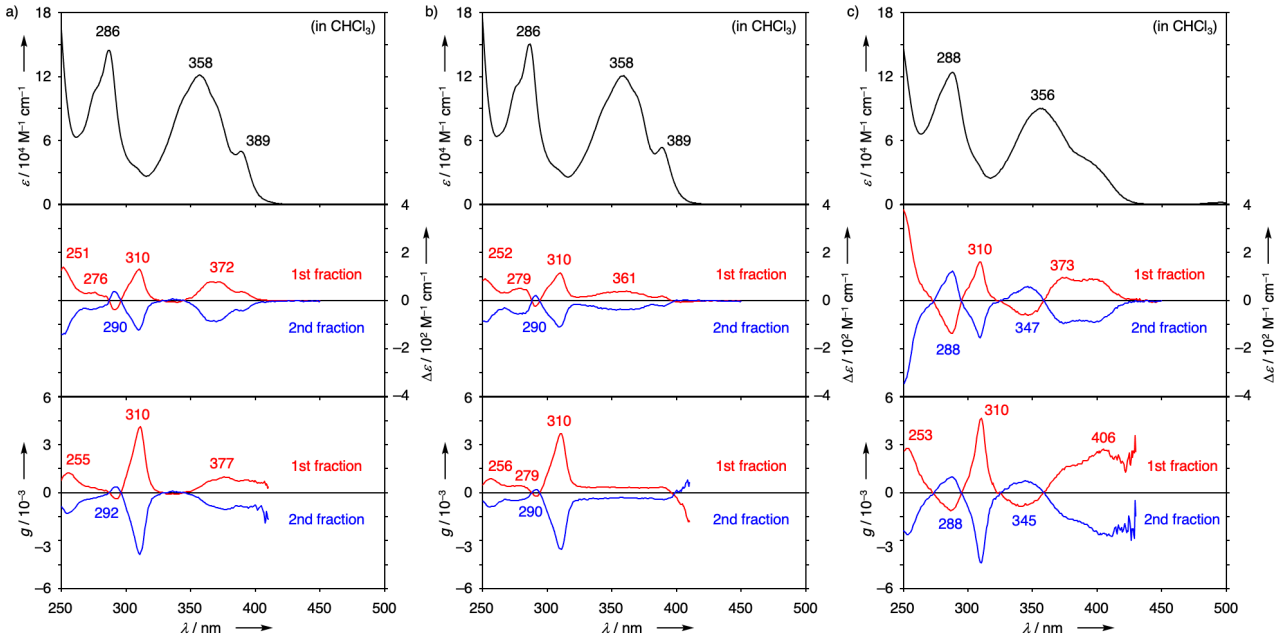

Fig. S6-2. UV/vis absorption (top) and CD (middle) spectra in $CHCl_3$, and dissymmetry factor plots (bottom, $g_{abs} = \Delta\varepsilon/\varepsilon$) of a) **10b**, b) **10c**, and c) **12**.

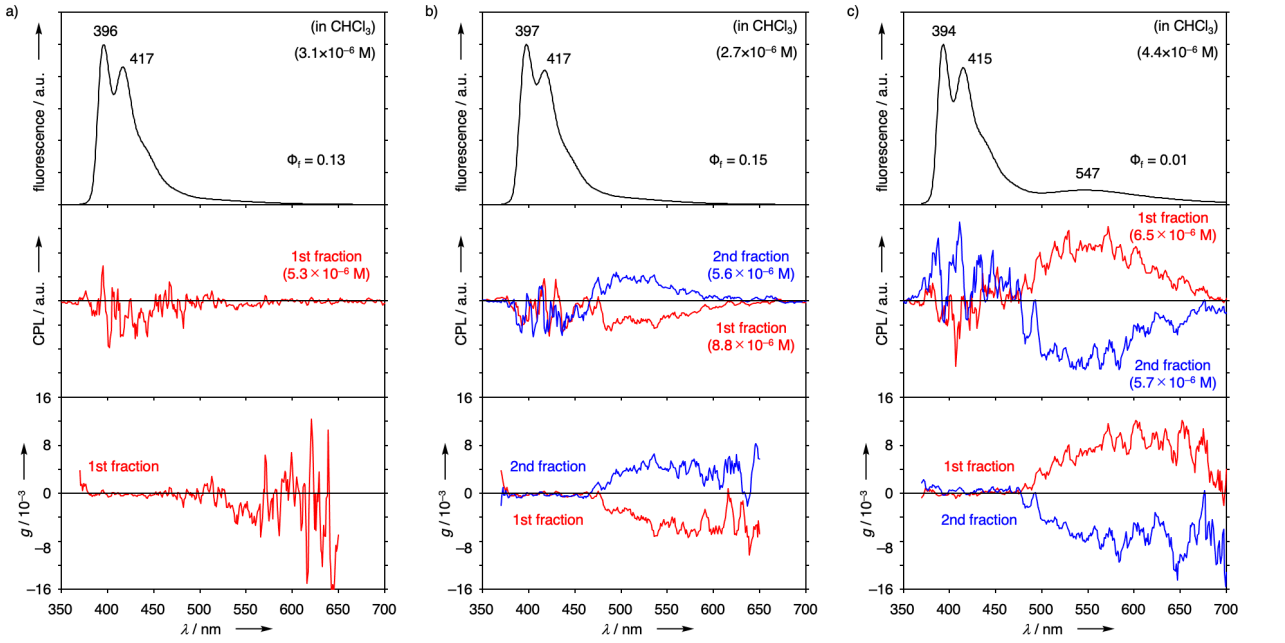

Fig. S6-3. Fluorescence (top) and CPL (middle) spectra in $CHCl_3$, and dissymmetry factor plots (bottom) of a) **10b**, b) **10c**, and c) **12**. Excitation wavelengths were set at 350 and 280 nm for fluorescence and CPL measurement respectively.

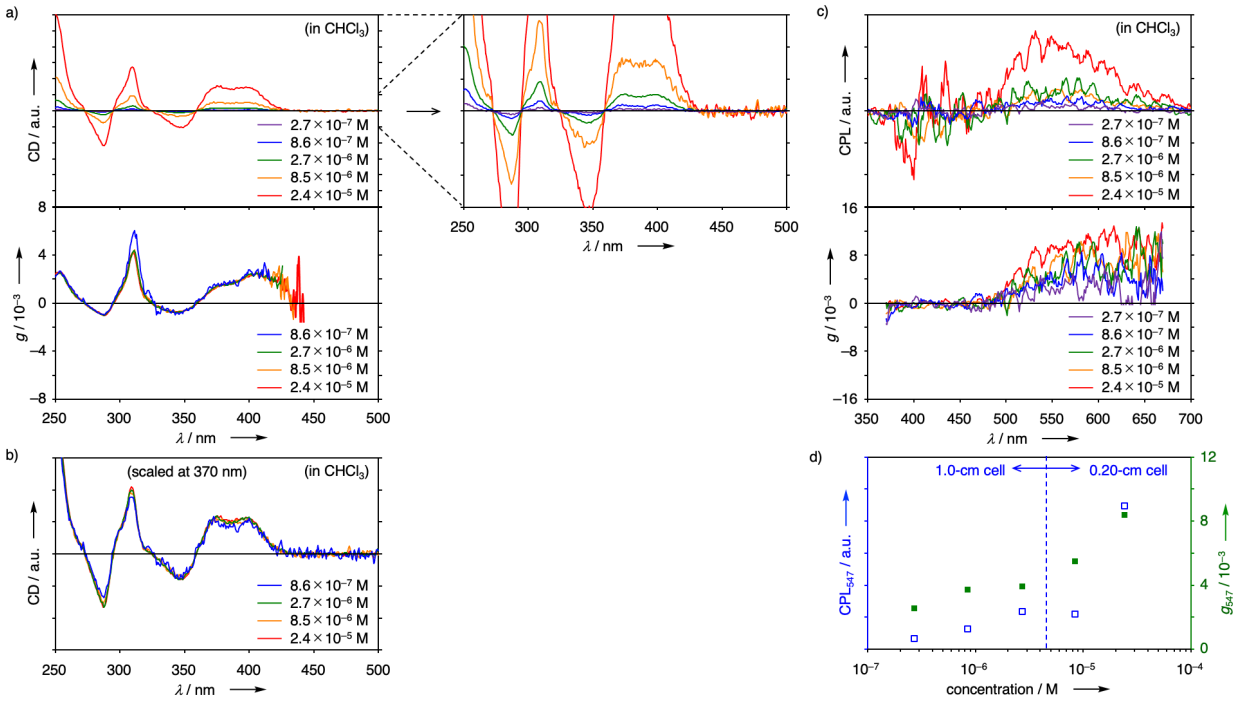

Fig. S6-4. a) Concentration-dependent CD (top) spectra and dissymmetry factor plots (bottom) of 1st fraction of **12** in $CHCl_3$. b) The spectra were scaled by the intensities at 370 nm. c) Concentration-dependent CPL (top) spectra and dissymmetry factor plots (bottom) of 1st fraction of **12** in $CHCl_3$. Excitation wavelengths were set at 280 nm. d) Plots of average CPL intensities over 537–557 nm (blue, left axis) and average dissymmetry factors over 537–557 nm (green, right axis) of 1st fraction of **12**. For concentrated solutions (8.5×10^{-6} and 2.4×10^{-5} M), 0.20-cm cell was used while 1.0-cm cell was used for the others.

7. References

[S1] K. Kato, Y. Kurakake, S. Ohtani, S. Fa, M. Gon, K. Tanaka and T. Ogoshi, *Angew. Chem. Int. Ed.* 2022, **61**, e202209222.

8. Additional information

To get insight into conformational equilibrium and mechanisms for excimer emission of **12**, low-temperature measurement was performed. In ^{1}H NMR spectra of 1.1×10^{-4} M solution (Fig. S8-1), new sets of peaks appeared one by one below 0 °C, without disappearance of the original signals at 25 °C. The new species were in slower equilibrium with the original one than ^{1}H NMR time scale and their intensified peaks suggested that they were thermodynamically stabilized at low temperature. At higher temperature, they were much unstable than the original species or cause severe peak broadening due to conformational equilibrium on the time scale. Although signal-to-noise ratio was rather poor, spectrum of 1.3×10^{-5} M solution (ca. 2–4 times of concentration for fluorescence and CPL measurement) at –20 °C was turned out not to be largely different from that of 1.1×10^{-4} M one, implying that new species were not dimer or higher aggregates but were monomers in different conformations and/or solvation states. For both 1.3×10^{-5} M and 1.6×10^{-6} M conditions, fluorescence spectral shapes at –20 °C were roughly unchanged from those at 25 °C while broad bands at around 550 nm were clearly intensified at –40 °C (Fig. S8-2). Between –20 and –40 °C, ^{1}H NMR spectra in Fig. S8-1 also showed large changes and therefore the same species were supposed to intensify the emission bond at around 550 nm by increasing contributions from intramolecular and/or intermolecular excimers.

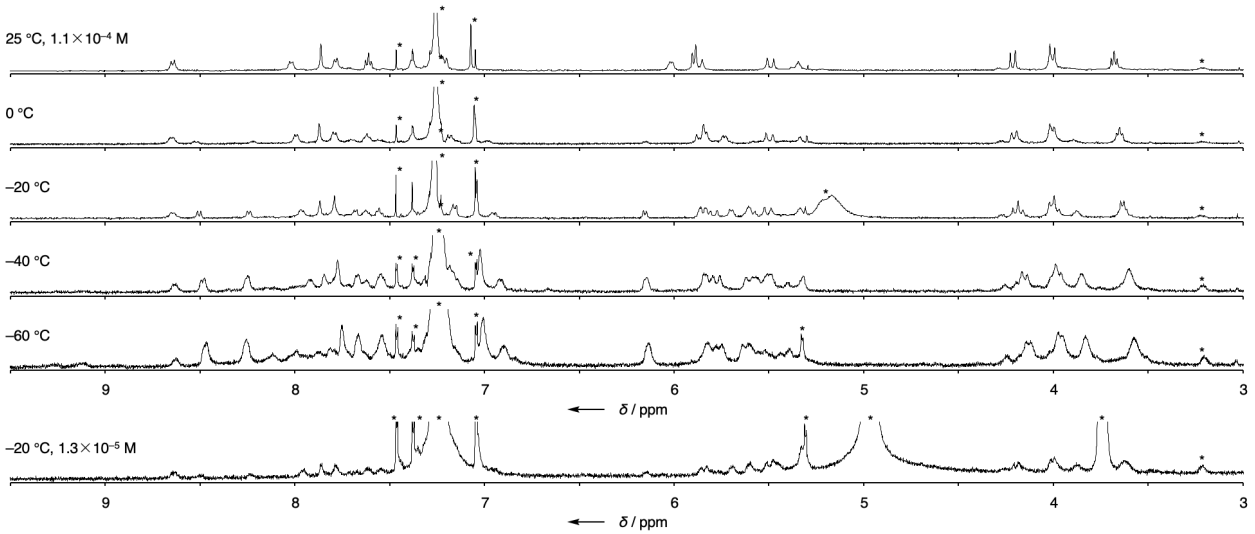

Fig. S8-1. Selected region of variable-temperature ^{1}H NMR spectra (top: 1.1×10^{-4} M) and ^{1}H NMR spectrum at –20 °C (bottom: 1.3×10^{-5} M) of **12** in $CDCl_3$. Peaks marked with * are due to residual solvents and impurities.

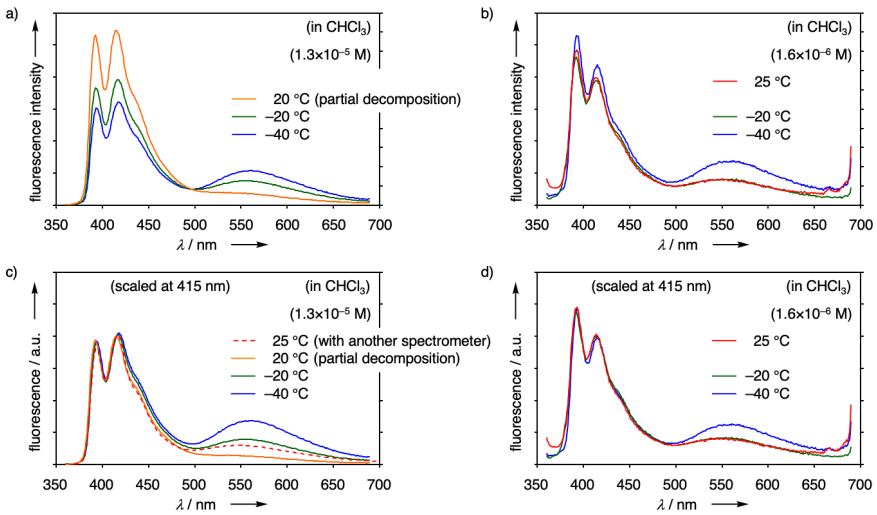

Fig. S8-2. Variable-temperature fluorescence spectra of **12** in $CHCl_3$ (excitation wavelength was set at 350 nm). The spectra were recorded at a) 1.3×10^{-5} M and b) 1.6×10^{-6} M, which were scaled by the intensities at 415 nm in figures c) and d) respectively. Unfortunately, **12** was not stable under repeated photoirradiation, like other per-alkoxy-substituted pillar[*n*]arenes, hampering detailed study using plots of peak intensities at different temperature.